Ir-catalyzed asymmetric hydrogenation with simple cyclohexane-based P/S ligands: In situ HP-NMR and DFT calculations for the characterization of reaction intermediates

Carlota Borràs, Maria Biosca, Oscar Pàmies,* and Montserrat Diéguez*

Departament de Química Física i Inorgànica. Universitat Rovira i Virgili. Campus Sescelades, C/ Marcel•lí Domingo, s/n. 43007 Tarragona, Spain.

Supporting Information Placeholder

ABSTRACT: We report a reduced but structurally valuable phosphite/phosphinite-thioether ligand library for the Ir-hydrogenation of 40 minimally functionalized alkenes, including relevant examples with poorly coordinative groups. We found that enantiomeric excesses are mainly dependent on the substrate structure and on some ligand parameters (i.e. the type of thioether/phosphorous moieties and the configuration of the phosphite group), whereas the substituents of the biaryl phosphite moiety had little impact. By tuning the ligand parameters we were able to find highly selective catalysts for a range of substrates (ee's up to 99%). These phosphite/phosphinite-thioether ligands have a simple backbone and thus yield simple NMR spectra that reduce signal overlap and facilitate the identification of relevant intermediates. Therefore, by combining HP-NMR spectroscopy and theoretical studies, we were also able to identify the catalytically competent Ir-dihydride alkene species, which made it possible to explain the enantioselectivity obtained.

INTRODUCTION

Over the last four decades, the increasing demand for enantiopure compounds for agrochemicals, pharmaceuticals and materials has stimulated the search for efficient methodologies for their preparation.[1] Because of its high selectivity and perfect atom-economic nature, transition-metal-catalyzed asymmetric hydrogenation is one of the most powerful and versatile approaches for preparing a wide range of enantiopure compounds.[1,2] This field has been dominated by the Rh/Ru-catalyzed asymmetric hydrogenation of substrates with a good coordination group close to the C-C double bond.[1-3] Today, an impressive range of ligands are being applied to transform a wide range of functionalized substrates. In contrast, the asymmetric hydrogenation of substrates that do not have an adjacent coordinative polar group – minimally functionalized olefins – is much less developed, despite the fact that it constitutes an easy way to create complex compounds from simple olefins.[4] In this respect, Ir-catalyzed asymmetric hydrogenation has emerged as an effective and easy method for reducing minimally functionalized olefins. Since Pfaltz applied Ir/phosphine-oxazoline PHOX chiral catalysts in 1998,[5] some of the most efficient reported chiral ligands have been mixed P-oxazoline ligands. Several successful phosphine/phosphinite/carbene-oxazoline ligands have been prepared by modifying the chiral backbone.[6] Our group has contributed to the Ir-hydrogenation of minimally functionalized olefins with an improved series of ligands. We have shown that phosphite groups improve the ligand's efficiency. Mixed phosphite-oxazoline ligands have been shown to be exceptionally effective, providing better substrate versatility than earlier Ir-phosphinite/phosphine-oxazoline catalysts.[7] Despite the advances achieved with Ir/P-oxazoline catalysts, the activity and enantioselectivity in the reduction of some relevant minimally functionalized olefins still need to be improved. To this end, research has progressed towards mixed ligands with groups that are more robust than oxazolines (pyridines,[8] amides,[9] thiazoles,[10] oxazoles,[11] etc.). In this context, we recently reported the use of non-N-donor mixed ligands – phosphite/phosphinite-thioether – in the enantioselective Ir-catalyzed reduction of minimally functionalized olefins.[12] The coordination of the thioether moiety to the iridium not only exerts steric and electronic effects by means of the change in the thioether groups, but also creates a new stereogenic center with a substituent that is very close to the iridium atom and therefore strongly shields one of the faces of the coordination sphere. In this context, two families of Ir/P-S catalysts were shown to hydrogenate a large variety of olefins with enantioselectivities comparable to the best ones reported to date.[12b,c] Despite this success, the performance of this new class of ligands must be further studied for this process by screening new readily accessible thioether-containing ligands and studying the species responsible for the catalytic performance under hydrogenation conditions. No experimental studies of the mechanism and the nature of the relevant catalytic intermediates under hydrogenation conditions have yet been carried out. The mechanistic proposals using phosphorus-thioether ligands are based on our previous work using DFT investigation.[12c] Therefore, in this paper we report a reduced but structurally valuable library of phosphite/phosphinite-thioether ligands **L1**-**L2a**-**g**[13] (Figure 1) for the Ir-hydrogenation of 40 minimally functionalized alkenes, including some specific examples with poorly coordinative groups. We also investigated the key

iridium intermediate complexes under hydrogenation conditions to explain the origin of the enantioselectivity. By combining high pressure NMR (HP-NMR) spectroscopy and theoretical studies we were able to identify the catalytically competent Ir-dihydride alkene species.

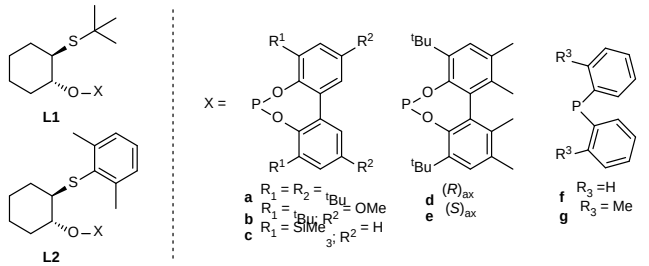

Figure 1. Phosphite/phosphinite-thioether ligands **L1**-**L2a**-**g**.

Phosphite/phosphinite-thioether ligands **L1**-**L2a**-**g** have been selected for this work because they have the following advantages: (a) they are synthesized in only two steps from commercially accessible cyclohexene oxide; (b) they benefit from the robustness of the thioether group; (c) a simple tuning of the thioether and phosphite/phosphinite moieties (**a**-**g**) provides control over the chiral cavity; and (d) their backbone is simple, thus yielding simple NMR spectra that reduce the overlap signals and facilitate the identification of relevant intermediates by HPNMR. For the purpose of this work, only two thioether substituents, *tert*-butyl and 2,6-dimethylphenyl, were used because previous work with Ir/P-thioether catalysts showed that these bulky substituents made it possible to achieve high enantioselectivities.[12b,c]

RESULTS AND DISCUSSION

Synthesis of ligands

The synthesis of ligands **L1**-**L2a**-**g** is shown in Scheme 1. The new ligands **L1**-**L2a**-**e** and **L2f**,**g** are prepared in only two steps from readily available cyclohexene oxide. The first step (Scheme 1, step (a)) consists of the enantioselective desymmetrization of cyclohexene oxide with the corresponding thiol using (*R*)-GaLibis(binaphtoxide) complex (GaLB-(*R*)), in keeping with Shibasaki's method.[14] Desymmetrization using *tert*-butylthiol provided the desired cyclohexanol-thioether **1** in >99% ee.[13a,b] However, desymmetrization using 2,6-dimethylbenzenethiol led to poor enantiocontrol (43% ee). Further enantiomer resolution by semipreparative chiral HPLC gave access to both enantiomers of the corresponding hydroxyl-thioether (**2** and *ent*-**2**). In the last step of the ligand synthesis process (Scheme 1 step (b)), cyclohexanol-thioether intermediates **1**-**2** were functionalized with different phosphite (**a**-**e**) or phosphinite moieties (**f**-**g**). Therefore, treating enantiopure hydroxyl-thioethers **1**-**2** with 1 equiv. of either the appropriate *in situ* formed phosphorochloridite ($ClP(OR)_2$, $(OR)_2$=**a**-**e**) or the required chlorophosphine ($ClPR_2$, R= **f**-**g**) provided the desired phosphite-thioether (**L1**-**L2a**-**e**) and phosphinite-thioether (**L1**-**L2f**-**g**) ligands.

All ligands were isolated in good yields as white solids (phosphite-thioether ligands **L1**-**L2a**-**e**) or colorless oils (phosphinite-thioether ligands **L1**-**L2f**-**g**) after purification on neutral alumina. They were found to be stable in air and resistant to hydrolysis, so they were further manipulated and stored in air. The elemental analyses and mass spectrometry were in agreement with the assigned structures. The ligands were also further characterized by $^{31}P\{^1H\}$, ^1H and $^{13}C\{^1H\}$ NMR spectroscopy. The spectral assignments were based on information from bidimensional ^1H-^1H and ^{13}C-^1H experiments. The $^{31}P\{^1H\}$ NMR spectra showed one singlet for each compound. The expected diastereoisomeric mixtures using tropoisomeric biphenyl phosphite moieties (**a**-**c**) were not detected by low-temperature $^{31}P\{^1H\}$ NMR, which is consistent with the fast ring inversions in the biphenylphosphorus moieties on the NMR time-scale.[15] ^1H and $^{13}C\{^1H\}$ NMR spectra showed the expected pattern for the cyclohexane backbone and the phosphite/phosphinite moieties. Concerning the protons of the cyclohexane ring, we found the signals of the corresponding diastereomeric methylene protons and the expected two signals for the methine protons. The methine protons adjacent to the sulfur atom appear at a lower chemical shift than the methine protons adjacent to the oxygen atom because the sulfur atom is less electron withdrawing than the oxygen atom. Finally, the ^1H and $^{13}C\{^1H\}$ NMR spectra also showed the expected pattern for the thioether groups.

Scheme 1. Synthesis of ligands L1-L2a-g.

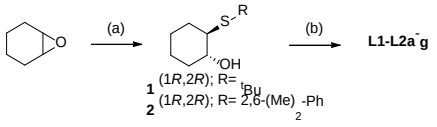

(a) GaLB-(*R*), RSH, toluene, molecular sieves 4 Å. For compounds **2** and *ent*-**2** semipreparative chiral HPLC was further needed; (b) $ClP(OR)_2$, Py, toluene or $ClPR_2/NEt_3$/toluene.

Synthesis of Ir-catalyst precursors

The reaction of the corresponding phosphite/phosphinite-thioether ligand **L1**-**L2a**-**g** with $[Ir(\mu\text{-}Cl)(cod)]_2$ in dichloromethane for one hour followed by *in situ* chlorine abstraction with $NaBAr_F$ produced the desired cationic catalyst precursors $[Ir(cod)(\mathbf{L1}\text{-}\mathbf{L2a}\text{-}\mathbf{g})]BAr_F$ (**3**-**12**; Scheme 2). These complexes were obtained in excellent yields and in pure form as orange-red solids. They were stable to air, so they were further manipulated and stored in air.

Scheme 2. Synthesis of $[Ir(cod)(L1\text{-}L2a\text{-}g)]BAr_F$ (3-12).

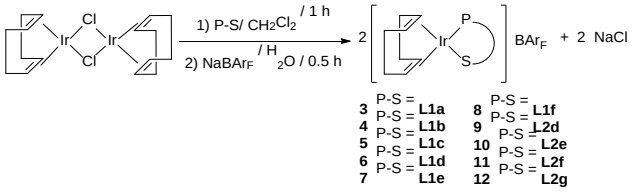

The complexes were characterized by elemental analysis, mass spectrometry and $^{31}P\{^1H\}$, ^1H and $^{13}C\{^1H\}$ NMR spectroscopy. For all complexes, the elemental analysis of C, H and S matched with the expected stoichiometry. The TOF-MS (ESI+) spectra show the highest ions at m/z, which correspond to the loss of the non-coordinated BAr_F anion from the mononuclear species $[Ir(cod)(\mathbf{L1}\text{-}\mathbf{L2a}\text{-}\mathbf{g})]BAr_F$. The $^{31}P\{^1H\}$ NMR spectra exhibited a sharp signal in all cases. However, for complexes **3**-**5**, the ^{31}P VT-NMR spectra (+35 °C to -80 °C) showed that the signals became broader when the temperature was lowered. This behavior has been attributed to the tropoisomerization of the biphenyl phos-

phite moieties (**a**-**c**), which led to a mixture of diastereoisomeric species in solution. This is supported by the fact that the $^{31}P\{^{1}H\}$ VT-NMR spectra of related complexes containing ligands with enantiomerically pure biphenyl moieties (**L1**-**L2d**-**e**) showed a single isomer in all cases, which rules out the possibility of the S-coordination being responsible for the diastereoisomeric species in complexes [Ir(cod)(**L1a**-**c**)]BAr_F.

Crystals suitable for X-ray diffraction analysis of the [Ir(**L1a**)(cod)]BAr_F complex were obtained by means of the slow diffusion of diethyl ether in a chloroform solution (Figure 2). It should be pointed out that only the diastereoisomer containing an *R*-disposition of the biaryl phosphite group crystallized out of the two observed diastereoisomers in solution (see above).

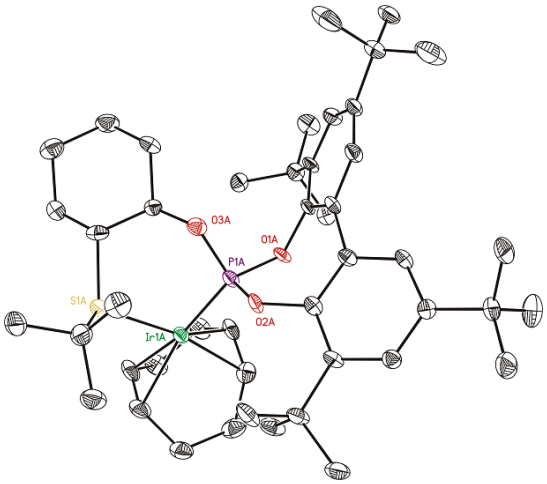

Figure 2. X-Ray structure of [Ir(**L1a**)(cod)]BAr_F complex **3** (hydrogens and BAr_F anion have been omitted for clarity).

The crystal structure clearly indicates the bidentate coordination of the P,S ligand through both donor atoms with a twist-boat conformation of the chelate ring. As expected, the large variations in the Ir-carbon bond distances *trans* the phosphite and thioether (c.a. 0.1 Å) point to the difference in *trans* influence between the two donor groups. The structure also shows a pseudoaxial disposition of the thioether substituent as previously observed by the analogue rhodium complex ([Rh(cod)(**L1f**)]BF_4).[13c] However, this behavior contrasts with the pseudoequatorial disposition of the thioether substituent in our previous Ir-structures containing arylglycidol-derived phosphite-thioether ligands, which also form a six-membered chelate ring.[12c] For this latter case, Ir/phosphite-thioethers catalysts have always provided much lower enantioselectivities in the reduction of minimally functionalized olefins than related Ir/phosphinite-thioether analogues, in which the thioether substituent adopts a pseudoaxial disposition. This, together with the fact that phosphite-thioether ligand reported in the present paper provided high enantioselectivities in several substrates (see below), could indicate that the disposition of the thioether substituent in the catalyst precursors has a relevant effect on the stereochemical outcome of the reaction.[16]

Asymmetric hydrogenation

Initially we tested the capacity of ligands **L1**-**L2a**-**g** by applying them in the reduction of the trisubstituted substrate **S1** model (Table 1). Excellent activities were obtained in all cases. However, the value of enantioselectivity depended on the type of thioether/phosphorous moieties and the configuration of the phosphite group, while the substituents of the biaryl phosphite moiety had little impact.

The effect on enantioselectivity of replacing the phosphite moiety with a phosphinite group depends on the thioether substituent. Thus, while for ligands **L1**, containing a *tert*-butyl thioether substituent, the addition of a phosphinite led to lower enantioselectivities (Table 1, entries 5 vs. 6), enantioselectivities increased for ligands **L2** with a 2,6-dimethylphenyl group (Table 1, entries 8 vs. 9). The results also show that a chiral phosphite moiety is needed for high enantioselectivity (entries 1-3 vs. 4-5). This indicates that, in contrast to previous xylofuranoside-based thioether-phosphite ligands,[12b] the simple cyclohexane-backbone is not able to control the tropoisomerization of the biaryl phosphite groups (**a**-**c**) in the active species, as has been found for [Ir(cod)(**L1a**-**c**)]BAr_F precatalysts (see above). Therefore, it is not surprising that low enantioselectivities were obtained for this substrate with Ir/**L1a**-**c** catalysts (entries 1-3). We also found a cooperative effect between the configuration of the cyclohexane-backbone and the configuration of the biaryl phosphite group (entries 4, 5, 7 and 8). This led to a matched combination with ligands containing an *S*-biaryl phosphite moiety (**e**; entries 5 and 8). The best enantioselectivity was therefore obtained with ligand **L1e** (ee's up to 86%; entry 5).

We also performed this reaction at a low catalyst loading (0.25 mol%) using Ir/**L1e**, which provided the best result, and enantioselectivity was maintained (Table 1, entry 11). Advantageously, the use of propylene carbonate (PC) as an environmentally friendly alternative solvent[17] to dichloromethane didn´t affected the stereochemical outcome of the reaction (entry 12).

Table 1. Ir-catalyzed hydrogenation of S1 using ligand library L1-L2a-g.[a]

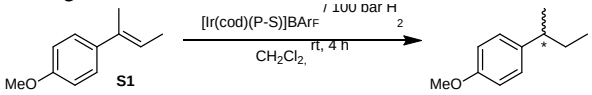

Entry	Ligand	% Conv[b]	% ee[b]
1	**L1a**	100	19 (*R*)
2	**L1b**	100	18 (*R*)
3	**L1c**	100	18 (*R*)
4	**L1d**	100	42 (*S*)
5	**L1e**	100	86 (*R*)
6	**L1f**	100	60 (*R*)
7	**L2d**	100	5 (S)
8	**L2e**	100	36 (*R*)
9	**L2f**	100	69 (*R*)
10	**L2g**	100	61 (*R*)
11[c]	**L1e**	100	86 (*R*)
12[d]	**L1e**	81	85 (*R*)

[a] Reactions carried out using 0.5 mmol of **S1** and 2 mol% of Ir-catalyst precursor. [b] Conversion and enantiomeric excesses determined by chiral GC. [c] Reaction carried out using 0.25 mol% of Ir-catalyst precursor. [d] PC as solvent.

To further establish the scope of Ir/**L1**-**L2a**-**g** catalysts, we chose a representative family of substrates, some of which contain neighboring polar groups. The results are summarized in Figure 3 (for a full set of results see Supporting Information). We found that the ligand parameters must be selected specifically for each substrate with the aim of obtaining the highest enantioselectivity. We initially considered the reduction of substrates **S2**-**S3**, which are related to **S1**. We found that enantioselectivities are relatively unaffected by varying the electronic and steric properties of the substrate (ee's between 85% and 92%). For both substrates the highest enantioselectivities were also obtained with Ir/**L1e** catalyst. The reduction of more challenging *Z*-isomers (model **S4** and **S5**), which are hydrogenated much less enantioselectively than *E*-isomers, also proceeded smoothly. We were pleased to see that for the more demanding *Z*-substrate **S5**, enantioselectivity (87% ee) was higher than for the *Z*-**S4** model.

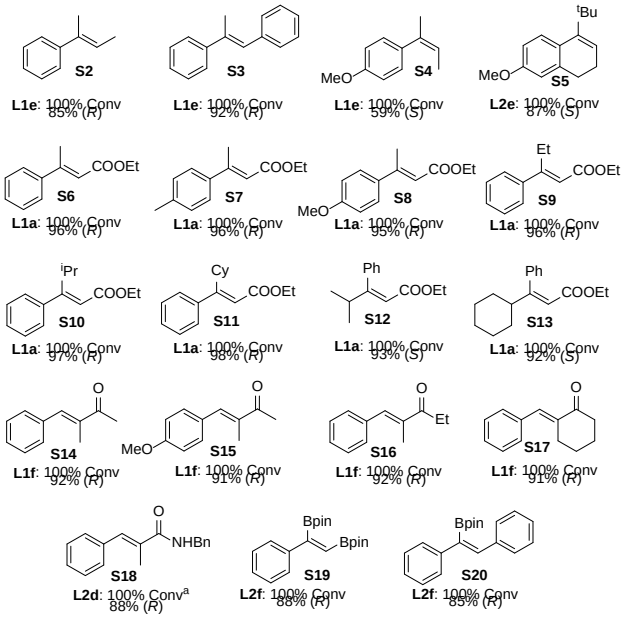

Figure 3. Asymmetric hydrogenation of trisubstituted substrates **S2**-**S20**. Reaction conditions: 1 mol % catalyst precursor, CH_2Cl_2 as solvent, 100 bar H_2, 4 h. [a] Reaction carried out for 18 h.

We then went on to study the reduction of a range of key trisubstituted olefins with poorly coordinative groups. Their hydrogenation is of particular importance because they can be further converted into relevant intermediates for synthesizing more complex chiral molecules. Interestingly, the hydrogenation of a very large series of α,β-unsaturated esters **S6**-**S13** proceeded with high enantioselectivities (ee's up to 98%), comparable to the best reported to date.[18] However, unlike previous **S1**-**S4** substrates, the effect of the ligand parameters on enantioselectivity is slightly different. Therefore, regardless of the thioether substituent, the presence of a biaryl phosphite moiety is highly beneficial and the tropoisomerization of the flexible biaryl phosphite moieties (**a**-**c**) is efficiently controlled (see Supporting Information). The best enantioselectivities were obtained using the Ir/**L1a**-**c** and Ir/**L1e** catalytic systems. Advantageously, the ee's were independent of the electronic nature of the substrate phenyl ring (**S6**-**S8**) and the steric nature of the alkyl substituent (**S6**, **S9**-**S11**). Also noteworthy were the high enantioselectivities obtained using more demanding *Z*-isomers (**S12** and **S13**). Being able to reduce such a range of α,β-unsaturated esters with these high ee's is highly significant because the resulting chiral carboxylic ester derivatives are present in many relevant products. This method is a more sustainable way to prepare these chiral carboxylic esters than other regular methodologies.[19] Another relevant set of substrates that is receiving much consideration are the α,β-unsaturated enones. In the reduction of a range of α,β-unsaturated enones **S14**-**S17**, the highest enantioselectivities (ee's up to 92%) were obtained with Ir-**L1f** catalyst, which contains a diphenylphosphinite moiety with a *tert*-butyl thioether substituent. The reduction of these kinds of olefins is an elegant route for producing ketones with a chiral center in the α position of the carbonyl moiety. Nevertheless, they have been less investigated and hydrogenated with less success than other trisubstituted olefins.[20]

These last results encouraged us to move on to the hydrogenation of other difficult olefins, such as enamide **S18**[21] and alkenylboronic esters **S19**-**S20**.[22] Few catalysts can afford high enantioselectivities for these alkenes, so it was noteworthy that we could reach high enantioselectivities in all of them by carefully modification of the ligand parameters. In the reduction of enamide **S18**, the highest enantioselectivities (up to 88%) were therefore achieved using [Ir(cod)(**L2d**)]BAr_F, while for alkenylboronic esters the best enantioselectivities (ee's up to 85%) were obtained with [Ir(cod)(**L2f**)]BAr_F. The reduction of enamides and alkenylboronic esters is also of great interest because hydrogenated products can easily been transformed into high-value compounds such us benzylic acid derivatives and chiral boron compounds.

Finally, we focused on the reduction of a more demanding type of substrate: 1,1-disubstituted olefins. Unlike trisubstituted olefins, 1,1-disubstituted olefins have not been successfully hydrogenated until very recently.[4a,e,h] This is because most of the successful catalysts developed for the reduction of trisubstituted substrates fail either to control the face-selective coordination of the less hindered disubstituted substrate or to suppress the isomerization of the olefin that leads to the formation of the more stable *E*-trisubstituted substrates, which in turn form the opposite enantiomer when hydrogenated. With the aim of evaluating the efficiency of ligands **L1**-**L2a**-**g** in hydrogenating this kind of substrate, we first studied the reduction of the model substrate **S21**. The results are shown in Table 2. We found that the substituents of the biaryl phosphite moiety have little impact on selectivity and that the presence of a chiral phosphite moiety (**d**-**e**) is needed for high enantioselectivity. However, in contrast to trisubstituted olefins, the best enantioselectivity was obtained with the ligand containing an *R*-biaryl phosphite moiety and 2,6-Me_2-C_6H_3 thioether substituent (ligand **L2d**, ee's up to 97%; entry 7). Interestingly, we also found that the configuration of the biaryl phosphite moiety controls the sense of enantioselectivity; therefore, both enantiomers of the reduction product can be obtained in high enantioselectivities under mild reaction conditions (entries 7 and 8).

Table 2. Ir-catalyzed hydrogenation of S21 using ligand library L1-L2a-g.[a]

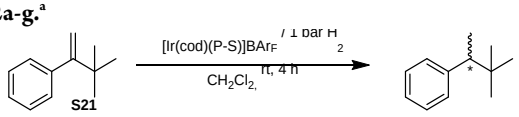

Entry	Ligand	% Conv[b]	% ee[b]
1	**L1a**	100	30 (*S*)
2	**L1b**	100	28 (*S*)
3	**L1c**	100	27 (*S*)
4	**L1d**	100	90 (*S*)
5	**L1e**	100	85 (*R*)
6	**L1f**	100	29 (*S*)
7	**L2d**	100	97 (S)
8	**L2e**	100	90 (R)
9	**L2f**	100	65 (S)
10	**L2g**	100	84 (S)

[a] Reactions carried out using 0.5 mmol of **S21** and 2 mol% of Ir-catalyst precursor.[b] Conversion and enantiomeric excesses determined by chiral GC.

The scope of Ir/**L1**-**L2a**-**g** catalysts was further studied by using other 1,1-disubstituted substrates (Figure 4, **S22**-**S40** and Supporting Information for a full set of results).

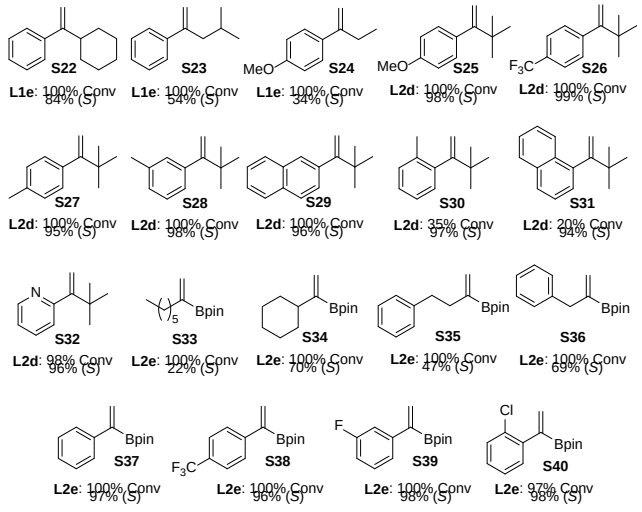

Figure 4. Asymmetric hydrogenation of 1,1-disubstituted olefins **S22**-**S40**. Reaction conditions: 1 mol % catalyst precursor, CH_2Cl_2 as solvent, 1 bar H_2, 4 h.

Our results with several α-alkylstyrenes with different sterically demanding alkyl groups (**S21**-**S24**) showed that enantioselectivity is influenced by the alkyl substituents (ee's ranging from 34% to 97%). This behavior may be due to a competition between direct hydrogenation and isomerization. In line with this, the hydrogenation of **S21** with a *tert*-butyl group, which cannot isomerize, provided the highest enantioselectivity. However, face selectivity problems cannot be ignored.[4 h] To address this issue, we carried out deuterium labeling experiments (Scheme 3) in which we reduced **S1** and **S24** with deuterium. In contrast to **S1**, the hydrogenation of **S24** led to the addition of deuterium not only at the expected positions (direct incorporation to the double bond), but also at the allylic position, which is in agreement of a competing isomerization pathway.[23] Accordingly, the mass spectra data of the corresponding deuterated product from **S24** showed species with more than two incorporated deuteriums (see Supporting Information).

Scheme 3. Deuterium labeling experiments of substrates S1 and S24.[a]

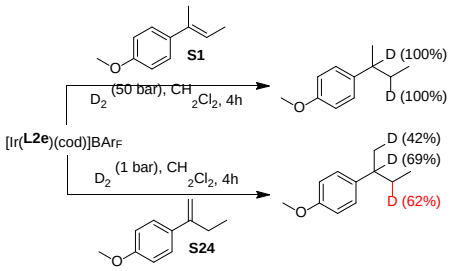

[a] The percentage of incorporation of deuterium atoms is shown in brackets. The results of the indirect addition of deuterium due to the isomerization process are shown in red.

We next screened a wide range of α-*tert*-butylstyrene type substrates (**S25**-**S31**) to evaluate how the steric and electronic properties of the aryl group of the substrate affected enantioselectivity. Advantageously, we found that enantioselectivity (ee's up to 99%) is relatively insensitive to changes in the electronic and steric properties of the aryl group. N-containing heterocycles are present in many relevant compounds such us pharmaceuticals and natural products. We were pleased to see that we could also obtained high enantioselectivities in both enantiomers of the reduction products of 2-(3,3-dimethylbut-1-en-2-yl)pyridine (**S32**).

Finally, due to the importance of chiral borane compounds, we wanted to see if the high enantioselectivities achieved in the reduction of trisubstituted alkenylboronic esters (Figure 3, substrate **S19**-**S20**) were retained for the even more challenging terminal analogues. The hydrogenation of such compounds using Ir-catalyst has recently emerged as a more sustainable alternative to the existing synthetic routes.[22a,b] However, high levels of enantioselectivity have only been obtained for alkyl-substituted terminal boronic esters such as **S33**-**S36**, and the hydrogenation of aryl-substituted boronic esters such as **S37** has yielded much lower enantioselectivities.[22a,b] Despite the moderate enantioselectivities achieved in the reduction of **S33**-**S36** using our new Ir-**L1**-**L2a**-**g** catalytic systems, we were pleased to find that a range of aryl-substituted terminal boronic esters **S37**-**S40** could be efficiently reduced using the Ir-**L2e** catalytic system. Interestingly, the substitution pattern in the aryl ring did not affect the stereochemical outcome of the reaction. This constitutes an important finding that overcomes the limitations previously encountered in the reduction of terminal aryl-substituted boronic esters and nicely complements the current state of the art.

In summary by efficiently selecting the ligand parameters of this reduced and simple readily available phosphite/phosphinite-thioether ligand family, we could obtain highly selective catalysts for a range of substrates, with enantioselectivities comparable in most cases to the best ones reported.

Mechanistic studies: study of reaction intermediates by in situ HP-NMR and theoretical studies

Computational and experimental research with P,N- and C,N-ligands showed that the hydrogenation of minimally functionalized olefins proceeds via and Ir^{III}/Ir^{V} migratory-insertion/reductive-elimination catalytic cycle.[24] Very recently, Pfaltz's group, based on

mechanistic studies under hydrogenation conditions, was able to detect the Ir(III) dihydride alkene intermediates responsible for the catalytic performance for the first time.[25] They found that, similarly to the classical Halpern-mechanism for asymmetric hydrogenation with Rh-catalysts, the minor intermediate, which is less stable, is converted to the major product enantiomer.

Similarly, our previous DFT investigations using Ir-P/S ligands also agree with Ir^{III}/Ir^{V} pathway, with migratory insertion of the hydride as an enantioselective-determining step.[12c] However, there is a lack of experimental evidences to support the calculations. On the basis of these previous studies and in an effort to rationalize the enantioselectivity achieved with the Ir-P/thioether catalysts reported in this manuscript, we performed an HP-NMR study of the iridium intermediates formed under hydrogenation conditions, with the aim of identifying the catalytically competent Ir-dihydride alkene species.

For this study, we initially investigated the oxidative addition of hydrogen to the iridium catalyst precursors $[Ir(cod)(P\text{-}S)]BAr_F$ (P-S = **L2f**, *ent*-**L2d** and **L2e**; Scheme 4). As models, we took complexes containing phosphinite-thioether ligand **L2f** and the phosphite-thioether ligands *ent*-**L2d** and **L2e**, respectively. These ligands contain different P-donor groups that can provide insight into their previously observed substantial effect on enantioselectivity (see above).

Scheme 4. Oxidative addition of H_2 to $[Ir(cod)(P\text{-}S)]BAr_F$ complexes 11, *ent*-9 and 10.

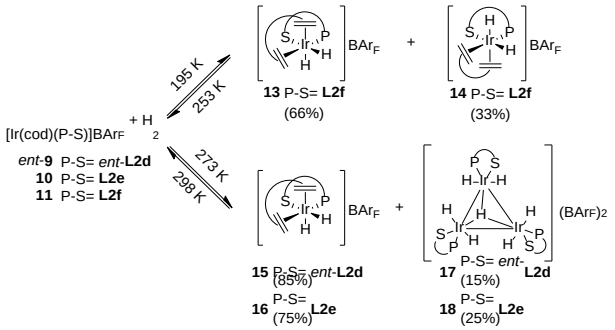

Bubbling H_2 in a CD_2Cl_2 solution of $[Ir(cod)(\mathbf{L2f})]BAr_F$ (**11**) at -78 °C led to the formation of two dihydride species **13** and **14** in a 2:1 ratio (Scheme 4), which are unstable when warming up. The equilibrium shifts back to the starting olefin complex **11** at -20 °C. Both isomers of $[Ir(H)_2(cod)(\mathbf{L2f})]BAr_F$ showed small phosphorus-hydride coupling constants ($^2J_{P\text{-}H} \leq 21.2$ Hz) that indicate that all the hydrides are *cis* to the phosphorus atom (Table 3).[13c,26]

Table 3. $^{31}P\{^1H\}$ and ^1H NMR data at the hydride region of dihydride species $[Ir(H)_2(cod)(\mathbf{L2f})]BAr_F$ (13 and 14), $[Ir(H)_2(cod)(\mathbf{ent\text{-}L2d})]BAr_F$ 15 and $[Ir(H)_2(cod)(\mathbf{L2e})]BAr_F$ 16.

Compound	H^a	H^b	$^{31}P\{^1H\}$
$[Ir(H)_2(cod)(\mathbf{L2f})]BAr_F$ (**13**)	-12.2 (d, $^2J_{P\text{-}H}$= 18 Hz)	-14.4 (d, $^2J_{P\text{-}H}$= 16.8 Hz)	86.2 (s)
$[Ir(H)_2(cod)(\mathbf{L2f})]BAr_F$ (**14**)	-12.3 (d, $^2J_{P\text{-}H}$= 21.2 Hz)	-15.9 (d, $^2J_{P\text{-}H}$= 16.8 Hz)	87.5 (s)
$[Ir(H)_2(cod)(\mathbf{ent\text{-}L2d})]BAr_F$ (**15**)	-12.4 (d, $^2J_{P\text{-}H}$= 22.4 Hz)	-14.7 (s)	73.4 (s)
$[Ir(H)_2(cod)(\mathbf{L2e})]BAr_F$ (**16**)	-12.43 (d, $^2J_{P\text{-}H}$= 21.6 Hz)	-14.63 (s)	86.1 (s)

The 3D structure of both isomers of $[Ir(H)_2(cod)(\mathbf{L2f})]BAr_F$ were assigned by DFT and NMR studies. Table 4 shows the calculated DFT relative energies of the four possible isomers with all the hydrides *cis* to the phosphinite group. These four structures result from the up or down relative position of one of the hydrides and the two possible configurations at the sulfur center (the S atom becomes a stereogenic center upon coordination to the metal).

Table 4. Calculated energies (in kJ/mol) for dihydride complexes 13-16 containing ligands L2f, *ent*-L2d and L2e, respectively.

Intermediate	**L2f**	***ent*-L2d**	**L2e**
A *S* config on sulfur	0	0	0
B *R* config on sulfur	20	18	29
C *S* config on sulfur	25	27	35
D *R* config on sulfur	12	29	30

The DFT calculations indicate that the most stable isomer **13** corresponds to intermediate **A** in which the hydride *trans* to the olefin (H^a) is pointing down with an *S* configuration at the S atom (Figure 5a). The minor isomer **14** has been assigned to intermediate **D** with the hydride *trans* to the olefin (H^a) pointing up and an *R* configuration at the S atom (Figure 5a). The assignments of the major and minor isomers of $[Ir(H)_2(cod)(\mathbf{L2f})]BAr_F$ were further confirmed by NOE experiments. The major isomer **13** therefore showed NOE contacts between the hydride *trans* to the olefin and the methine proton adjacent to the P group, while for the minor isomer **14** this NOE interaction appeared with the methine proton adjacent to the thioether group (Figure 5b). The agreement between the NMR elucidation and the DFT calculations of structures of **13** and **14** validates the computational model used. The ob-

served results may be compared with those obtained from the oxidative addition of H_2 to [Ir(cod)(**L1f**)]SbF_6, whose ligand differs from (**11**) by a *tert*-butyl thioether group instead of a 2,6-dimethylphenyl thioether moiety.[13c] The use of Evans and colleagues' ligand leads to a single dihydride species with high thermal stability which has the same structure of the major isomer **13**.

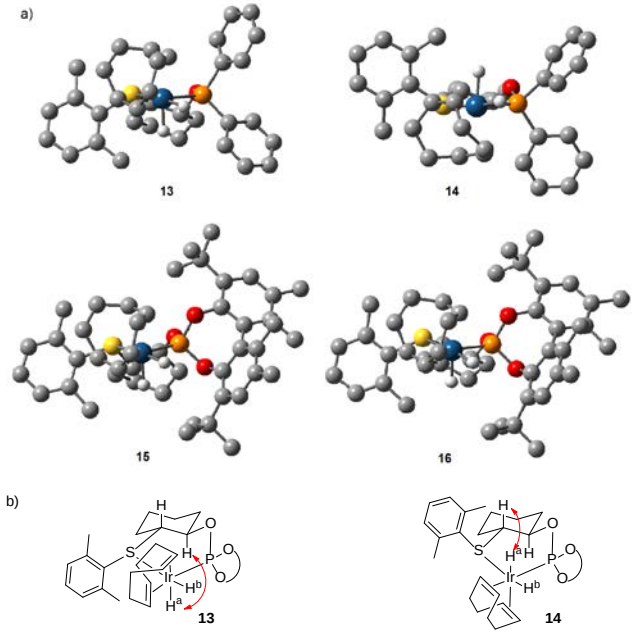

Figure 5. a) Calculated structures of dihydride [Ir(H)$_2$(cod)(P-S)]BAr_F complexes **13**-**16** (hydrogen atoms and BAr_F anion have been omitted for clarity). b) Relevant NOE contacts from the NOESY experiment of dihydride [Ir(H)$_2$(cod)(P-S)]BAr_F complexes **13** and **14**.

We next studied the oxidative addition of H_2 to [Ir(cod)(P-S)]BAr_F precursors containing phosphite-thioether ligands *ent*-**L2d** and **L2e** (compounds *ent*-**9** and **10**). Only one dihydride intermediate was detected for each and required up to 0 °C to push the equilibrium to the expected dihydride species (Scheme 4). The observed results contrast with [Ir(H)$_2$(cod)(**L2f**)]BAr_F where two dihydride species were observed and required -78 °C. Again, the NMR spectra of the dihydride intermediates of each complex indicated that they are *cis* to the phosphorus atom (Table 3). The final assignments of these dihydride intermediates were performed by DFT studies (Table 4). As observed for the previous diphosphinite analogue [Ir(H)$_2$(cod)(**L2f**)]BAr_F, dihydride compounds **15** and **16** correspond to intermediate **A** in which the hydride *trans* to the olefin (H^a) is pointing down with an *S* configuration at the S atom (Figure 5a). It should be noted, that at 0 °C the cyclooctadiene of the catalyst precursors *ent*-**9** and **10** also hydrogenated, resulting in the concomitant formation of other species, that have been assigned to catalytically inactive trinuclear iridium hydrido species [Ir$_3$(μ_3-H)(H)$_6$(P-S)$_3$](BAr_F)$_2$ **17** and **18** (Scheme 4).[27,28] These trinuclear iridium hydrido species **17** and **18** showed the expected pattern of the hydrides. Thus, for instance, for **17** the bridging μ_3 hydride signal appeared at -5.62 ppm as quadruplet due to the coupling with the three phosphorus atoms, while the terminal hydride resonances appeared at -13.58 ppm and at -33.72 ppm as a singlet and a broad signal, respectively. The hydride resonances for **18** appeared at -4.48, -14.53 and -36.94 ppm, respectively.

We next investigated the reactivity of iridium precatalysts [Ir(cod)(**L2f**)]BAr_F **11**, [Ir(cod)(*ent*-**L2d**)]BAr_F *ent*-**9** and [Ir(cod)(**L2e**)]BAr_F **10** with H_2 in the presence of an alkene (Scheme 5). The alkene used was (*E*)-1-methyl-4-(1-phenylprop-1-en-2-yl)benzene-D_5 **19**, in accordance with the methodology recently described by Pfaltz and colleagues.[25]

Scheme 5. Reactivity of [Ir(cod)(P-S)]BAr_F complexes with olefin 19 under hydrogenation conditions.

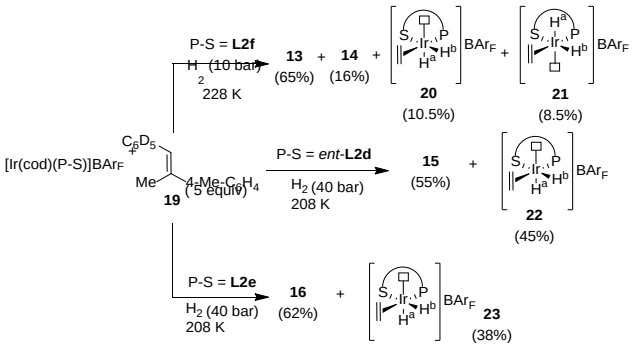

Under 10 bar of H_2 at -45 °C, the reaction of **11** with five equiv. of **19** led to the formation of four dihydride complexes in a ratio 6:1.5:1:0.8 (Scheme 5). The two most abundant complexes were unambiguously assigned to the two dihydrides **13** and **14** described above. The minor isomers were assigned to the elusive dihydride intermediate species [Ir(H)$_2$(**19**)(**L2f**)]BAr_F **20** and **21**, in which the alkene is coordinated (Table 5).

Table 5. $^{31}P\{^1H\}$ and ^1H NMR data at the hydride region of dihydride alkene species [Ir(H)$_2$(19)(L2f)]BAr_F (20 and 21), [Ir(H)$_2$(19)(*ent*-L2d)]BAr_F 22 and [Ir(H)$_2$(19)(L2e)]BAr_F 23.

Compound	H^a	H^b	$^{31}P\{^1H\}$
[Ir(H)$_2$(**19**)(**L2f**)]BAr_F (**20**)	-28.52 (d, $^2J_{P\text{-}H}$= 26 Hz)	-16.41 (d, $^2J_{P\text{-}H}$= 17.2 Hz)	75.2 (s)
[Ir(H)$_2$(**19**)(**L2f**)]BAr_F (**21**)	-25.59 (d, $^2J_{P\text{-}H}$= 27.6 Hz)	-16.23 (d, $^2J_{P\text{-}H}$= 15.6 Hz)	84.1 (s)
[Ir(H)$_2$(**19**)(*ent*-**L2d**)]BAr_F (**22**)	-25.67 (d, $^2J_{P\text{-}H}$= 34.8 Hz)	-16.19 (s)	76.3 (s)
[Ir(H)$_2$(**19**)(**L2e**)]BAr_F (**23**)	-27.22 (d, $^2J_{P\text{-}H}$= 32.1 Hz)	-16.74 (d, $^2J_{P\text{-}H}$= 7.2 Hz)	77.4 (s)

The alkene coordination to iridium in these dihydride intermediate species **20** and **21** was verified by ^{1}H-NMR, which showed a significant low-frequency shift of the olefinic proton of the alkene **19** from 6.82 to *ca* 4.8 ppm. Interestingly, in the ^{1}H-NMR spectra of species **20** and **21** one of the hydrides appeared high-field shifted (between -25.6 and -28.5 ppm). This is characteristic of a hydride ligand positioned *trans* to the coordination site which is either vacant or engaged in a C-H agostic interaction.[25] As for [Ir(H)$_2$(cod)(**L2f**)]BAr_F complexes **13** and **14**, dihydride alkene intermediate species **20** and **21** also show a small phosphorus-hydride coupling constant ($^2J_{P\text{-}H} \leq$ 27.6 Hz), which indicates that all the hydrides are *cis* to the phosphorus atom. This behavior is not

unexpected because early theoretical calculations on Ir(III) dihydride alkene intermediates showed the alkene coordinated *trans* to the phosphorus donor group.[24]

On the other hand, the reaction of iridium precatalysts [Ir(cod)(*ent*-**L2d**)]BAr_F and [Ir(cod)(**L2e**)]BAr_F with five equiv. of **19** under optimized reaction conditions (40 bar of H_2 at -65 °C) led to the formation for each complex of two hydride species at a ratio of 1.2:1 and 1.6:1, respectively (Scheme 5). In both cases, the major isomers were assigned to the corresponding dihydride complexes [Ir(H)$_2$(cod)(P-S)]BAr_F **15** and **16**, whereas the minor isomers were attributed to [Ir(H)$_2$(**19**)(P-S)]BAr_F intermediate species (**22** and **23**) in which the alkene is coordinated (Table 5).

The assignments of the 3D structure of both isomers of [Ir(H)$_2$(**19**)(**L2f**)]BAr_F **20** and **21** and of the isomer of each complex of [Ir(H)$_2$(**19**)(*ent*-**L2d**)]BAr_F **22** and [Ir(H)$_2$(**19**)(**L2e**)]BAr_F **23** were performed by DFT studies. Unfortunately, due to signal overlap in the ^{1}H NMR, these studies could not be validated by NOE experiments. The DFT relative energies of the sixteen possible isomers with all the hydrides *cis* to the phosphinite/phosphite group are shown in Table 6. These isomers result from varying the relative position of one of the hydrides, the coordination of two enantiotopic olefin faces, the two possible configurations at the sulfur center and the relative position of the vacant site (up or down). The results indicate that the observed major (**20**) and minor (**21**) isomers of the olefinic dihydride intermediates [Ir(H)$_2$(**19**)(**L2f**)]BAr_F adopt structures **K** and **A**, respectively, while intermediates **22** adopts an **L** structure and intermediate **23** adopts an **K** structure.

Table 6. Calculated energies (in kJ/mol) for dihydride olefin complexes 20-23 containing ligands L2f, *ent*-L2d and L2e, respectively.

Intermediate	**L2f**	*ent*-**L2d**	**L2e**	Intermediate	**L2f**	*ent*-**L2d**	**L2e**
 **A** *R* config on sulfur	0.9	13.2	2.2	 **I** *R* config on sulfur	16.1	20.8	13.0
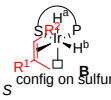 **B** *S* config on sulfur	16.2	21.7	20.3	 **J** *S* config on sulfur	15.4	19.3	21.4
 **C** *R* config on sulfur	48.3	11.8	12.0	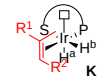 **K** *R* config on sulfur	0	12.9	0
 **D** *S* config on sulfur	26.5	6.7	24.1	 **L** *S* config on sulfur	5.7	0	7.3
 **E** *R* config on sulfur	-	44.4	32.0	 **M** *R* config on sulfur	-	33.3	25.8
 **F** *S* config on sulfur	35.4	33.5	49.2	 **N** *S* config on sulfur	17.8	19.7	22.6
 **G** *R* config on sulfur	18.3	29.9	30.1	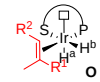 **O** *R* config on sulfur	18.9	31.1	31.1
 **H** *S* config on sulfur	36.1	36.9	47.3	 **P** *S* config on sulfur	32.8	32.5	37.1

With these mechanistic results in hand, we next screened precatalysts [Ir(cod)(**L2f**)]BAr_F **11**, [Ir(cod)(*ent*-**L2d**)]BAr_F *ent*-**9** and [Ir(cod)(**L2e**)]BAr_F **10** with substrate **19** under the conditions used for the HP-NMR analysis. The results are shown in Scheme 6. For precatalyst [Ir(cod)(**L2f**)]BAr_F **11** the configuration of the product obtained from hydrogenation is *R* (Scheme 6), which requires coordination of the substrate as determined for the minor isomer **21**. This result therefore indicates that the hydrogenation of substrate **19** with the Ir/**L2f** catalytic system follows the Halpern-type mechanism in which the less stable isomer **21** reacts faster than the major intermediate **20**, and it is converted into the major product enantiomer. The same behavior is obtained using precatalysts [Ir(cod)(*ent*-**L2d**)]BAr_F *ent*-**9** and [Ir(cod)(**L2e**)]BAr_F **10**. Thus, the configuration of the hydrogenated products are *R*, while the expected from the detected isomers of **22** and **23** is *S*.

Scheme 6. Asymmetric hydrogenation of 21 using precatalysts [Ir(cod)(L2f)]BAr$_F$ 11, [Ir(cod)(*ent*-L2d)]BAr$_F$ *ent*-9 and [Ir(cod)(L2e)]BAr$_F$ 10 under HP-NMR conditions.

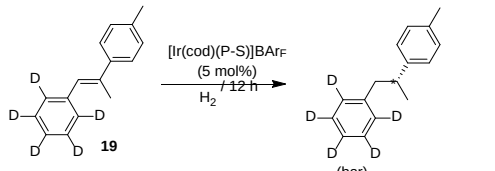

P-S	p_{H2} (bar)	T (K)	%ee
L2f	10	228	65 (*R*)
ent-**L2d**	40	208	8 (*R*)
L2e	40	208	34 (*R*)

From this we can conclude that in order to obtain the highest enantioselectivity the amount of the minor faster reacting isomer has to be enhanced and/or the energy difference, and therefore the reaction rates, between both TS resulting from the major and minor isomers observed has to be increased. Accordingly, the lowest enantioselectivities obtained with precatalysts [Ir(cod)(*ent*-**L2d**)]BAr$_F$ *ent*-**9** and [Ir(cod)(**L2e**)]BAr$_F$ **10** in comparison with [Ir(cod)(**L2f**)]BAr$_F$ **11** can been explained by the lower population of the faster reacting olefinic dihydride isomer.

CONCLUSIONS

We report a reduced but structurally valuable phosphite/phosphinite-thioether ligand library for the Ir-hydrogenation of 40 minimally functionalized alkenes, including some relevant examples with poorly coordinative groups. These phosphite/phosphinite-thioether ligands are synthesized in only two steps from commercially accessible cyclohexene oxide. They also benefit from the robustness of the thioether group and the additional control of the chiral cavity by tuning the thioether and phosphite/phosphinite moieties. With a simple tuning of these ligand parameters we developed highly selective catalysts for a range of substrates with enantioselectivities up to 99%, including a variety of olefins that have recently caught attention because their hydrogenated compounds can lead to high-value chemicals. Moreover, these catalysts extend the state-of-the-art with the successful reduction, for the first time, of terminal aryl-substituted boronic esters. It is also remarkable that these thioether-phosphite/phosphinite ligands have a simple backbone and thus their NMR spectra are simple, with reduced signal overlap, which facilitates the identification of relevant intermediates. Therefore, by combining HP-NMR spectroscopy and theoretical studies, we were able to identify the catalytically competent Ir-dihydride alkene species, which made it possible to explain the enantioselectivity obtained. We found that, similarly to the classical Halpern-mechanism for asymmetric hydrogenation with Rh-catalysts, the minor intermediate, which is less stable, is converted to the major product enantiomer.

EXPERIMENTAL SECTION

General considerations. All reactions were carried out using standard Schlenk techniques under an argon atmosphere. Commercial chemicals were used as received. Solvents were dried by means of standard procedures and stored under argon. ^{1}H, ^{13}C{^{1}H} and ^{31}P{^{1}H} NMR spectra were recorded using a Varian Mercury-400 MHz spectrometer. Chemical shifts are relative to that of $SiMe_4$ (^{1}H and ^{13}C{^{1}H}) as an internal standard or H_3PO_4 (^{31}P) as an external standard. ^{1}H and ^{13}C assignments were made on the basis of ^{1}H-^{1}H gCOSY, ^{1}H-^{13}C gHSQC and NOESY experiments. The GaLB-(*R*) solution was prepared in accordance with a method published in the literarure.[14] Phosphorochloridites were easily prepared in one step from the corresponding biphenols.[29] Enantiopure hydroxyl-thioether compound **1**,[13b] thioether-phosphinite ligand **L1f**[13b] and (*E*)-1-methyl-4-(1-phenylprop-1-en-2-yl)benzene-D5 **19**[25] were prepared as previously described.

Computational details. The geometries of all intermediates were optimized using the Gaussian 09 program,[30] employing the B3LYP[31] density functional and the LANL2DZ[32] basis set for iridium and the 6-31G* basis set for all other elements.[33] Solvation correction was applied in the course of the optimizations using the PCM model with the default parameters for dichloromethane.[34] The complexes were treated with charge +1 and in the single state. No symmetry constraints were applied. The energies were further refined by performing single point calculations using the above mentioned parameters, with the exception that the 6-311+G**[35] basis set was used for all elements except iridium, and by applying dispersion correction using DFT-D3[36] model. All energies reported are Gibbs free energies at 298.15 K and calculated as $G_{reported} = G_{6\text{-}31G^*} + (E_{6\text{-}311+G^{**}} - E_{6\text{-}31G^*}) + E_{DFT\text{-}D3}$.

Preparation of (1R, 2R)-2-(2,6-dimethylphenylthio)cyclohexanol (2). A mixture of a 0.05 M solution of GaLB-(*R*) (2.0 mL, 0.10 mmol) and powdered MS 4Å (200 mg) was stirred at room temperature for 30 min and then evaporated *in vacuo* to remove THF. Toluene (2.0 mL) and cyclohexene oxide (101 µL, 1.00 mmol) were added to the residue, and then 2,6-dimethylbenzenethiol (160 µL, 1.20 mmol) was added in one portion. The mixture was stirred at room temperature for 9 h, then diluted with diethyl ether (30 mL) and filtered over a celite pad. The filtrate was washed successively with 5% *aq*. citric acid (10 mL), sat. *aq*. $NaHCO_3$ (10 mL), and brine (10 mL), dried over $MgSO_4$ and then evaporated *in vacuo*. The residue was purified by flash chromatography (SiO_2, hexane/acetone (20:1)) to yield the desired thioether-alcohol as a mixture of enantiomers. Further enantiomeric resolution by using semipreparative chiral HPLC (Daicel CHIRACEL OD, 3% 2-propanol in hexanes, 5 mL·min^{-1}, 23 min (**2**)) gave access to desired enantiomer hydroxyl-thioether **2** as a white solid. Yield: 69 mg (29%). ^{1}H NMR (C_6D_6), δ: 1.16 (m, 1H, CH_2), 1.24 (m, 2H, CH_2), 1.31 (m, 1H, CH_2), 1.63 (m, 1H, CH_2), 1.73 (m, 1H, CH_2), 1.88 (m, 1H, CH_2), 2.12 (m, 1H, CH_2), 2.58 (s, 6H, CH_3-Ph), 2.63 (b, 1H, OH), 2.72 (m, 1H, CH-O), 3.56 (m, 1H, CH-S), 7.13 (b, 3H, CH=). ^{13}C NMR (C_6D_6), δ: 22.6 (CH_3), 24.2 (CH_2), 25.8 (CH_2), 32.5 (CH_2), 34.1 (CH_2), 56.4 (CH-O), 73.9 (CH-S), 128.3 (CH=), 132.0 (C), 143.5 (CH=). Anal. calcd. (%) for $C_{14}H_{20}OS$: C 71.14, H 8.53, S 13.56; found: C 71.07, H 8.56, S 13.48. MS HR-ESI [found 236.1232, $C_{14}H_{20}OS$ requires 236.1235].

General procedure for the preparation of the thioether-phosphite ligands L1-L2a-e. The corresponding phosphorochloridite (1.1 mmol) produced *in situ* was dissolved in toluene (5 mL) and pyridine (3.8 mmol, 0.3 mL) was added. The corresponding hydroxyl-thioether (1 mmol) was azeotropically dried with toluene (3x1 mL) and dissolved in toluene (5 mL) to which pyridine (3.8 mmol, 0.3 mL) was added. The solution was transferred slowly at 0 °C to the phosphorochloridite solution. The reaction mixture was stirred overnight at 80 °C, and the pyridine salts were removed by filtration. The evaporation of the solvent yielded a white foam, which was purified by flash chromatography in alumina (eluent: toluene/triethylamine – 100:1) to produce the corresponding ligand as a white solid.

L1a: Yield: 423 mg (67%). ^{31}P NMR (C_6D_6), δ: 146.3. ^{1}H NMR (C_6D_6), δ: 1.23 (b, 2H, CH_2), 1.26 (s, 9H, CH_3, S^{t}Bu), 1.34 (s, 9H, CH_3, ^{t}Bu), 1.38 (s, 9H, CH_3, ^{t}Bu), 1.55 (m, 1H, CH_2), 1.69 (m, 3H, CH_2), 1.72 (s, 18H, CH_3, ^{t}Bu), 1.84 (m, 2H, CH_2[1]), 2.38 (m, 1H, CH_2), 3.19 (b, 1H, CH-S), 4.75 (b, 1H, CH-O), 7.42 (m, 2H, CH=), 7.69 (m, 2H, CH=).^{13}C NMR (C_6D_6), δ: 20.2 (CH_2), 22.1 (CH_2), 29.2 (b, CH_2), 29.8 (b, CH_2), 30.9 (CH_3, S^{t}Bu), 31.1 (CH_3, ^{t}Bu), 31.2 (CH_3, ^{t}Bu), 31.3 (CH_3, ^{t}Bu), 34.2 (C, ^{t}Bu), 34.3 (C, ^{t}Bu), 35.3 (C, ^{t}Bu), 35.4 (C, ^{t}Bu), 43.0 (CH-S), 44.2 (C, S^{t}Bu), 76.7 (b, CH-O, $^2J_{C\text{-}P}$=7.7Hz), 123.9-146.2 (aromatic carbons). Anal. calcd. (%) for $C_{38}H_{59}O_3PS$: C 72.80, H 9.49, S 5.11; found: C 72.71, H

9.44, S 5.06. MS HR-ESI [found 649.3811, $C_{38}H_{59}O_3PS$ $(M\text{-}Na)^+$ requires 649.3815].

L1b: Yield: 410 mg (71%). ^{31}P NMR (C_6D_6), δ: 146.0. ^1H NMR (C_6D_6), δ: 1.22 (s, 9H, CH_3, S^{t}Bu), 1.32 (b, 2H, CH_2), 1.55 (s, 9H, CH_3, ^{t}Bu), 1.56 (s, 9H, CH_3, ^{t}Bu), 1.63 (b, 3H, CH_2), 1.83 (m, 1H, CH_2), 1.94 (m, 1H, CH_2), 2.31 (m, 1H, CH_2), 3.14 (b, 1H, CH-S), 3.31 (s, 3H, CH_3-O), 3.34 (s, 3H, CH_3-O), 4.73 (b, 1H, CH-O), 6.65-7.18 (4H, CH=). ^{13}C NMR (C_6D_6), δ: 20.1 (CH_2), 21.9 (CH_2), 29.4 (b, CH_2), 29.6 (b, CH_2), 30.8 (CH_3, ^{t}Bu), 30.9 (CH_3, ^{t}Bu), 35.1 (C, ^{t}Bu), 35.3 (C, ^{t}Bu), 43.0 (CH-S), 44.0 (C, S^{t}Bu), 54.6 (CH_3-O), 54.7 (CH_3-O), 76.6 (d, CH-O, $^2J_{C\text{-}P}$=8.6Hz), 113.0-155.9 (aromatic carbons). Anal. calcd. (%) for $C_{32}H_{47}O_5PS$: C 66.87, H 8.24, S 5.58; found: C 66.85, H 8.22, S 5.55. MS HR-ESI [found 597.2768, $C_{32}H_{47}O_5PS$ $(M\text{-}Na)^+$ requires 597.2774].

L1c: Yield: 343 mg (63%). ^{31}P NMR (C_6D_6), δ: 142.3. ^1H NMR (C_6D_6), δ: 0.44 (s, 9H, CH_3Si), 0.47 (s, 9H, CH_3Si), 1.13 (s, 9H, CH_3,S ^{t}Bu), 1.25 (m, 2H, CH_2), 1.48-1.72 (b, 5H, CH_2), 2.21 (m, 1H, CH_2), 2.97 (m, 1H, CH-S), 4.52 (m, 1H, CH-O), 7.03-7.42 (6H, CH=). ^{13}C NMR (C_6D_6), δ: 0.0 (CH_3Si), 0.1 (CH_3Si), 20.8 (CH_2), 22.5 (CH_2), 29.7 (b, CH_2), 30.4 (b, CH_2), 31.0 (CH_3,^{t}Bu), 43.0 (CH-S), 44.5 (C, S^{t}Bu), 76.9 (d, CH-O, $^2J_{C\text{-}P}$=3.1Hz), 124.5-155.2 (aromatic carbons). Anal. calcd. (%) for $C_{28}H_{43}O_3PSSi_2$: C 61.50, H 7.93, S 5.86; found: C 61.47, H 7.92, S 5.83. MS HR-ESI [found 569.2098, $C_{28}H_{43}O_3PSSi_2$ $(M\text{-}Na)^+$ requires 569.2101].

L1d: Yield: 399 mg (69%). ^{31}P NMR (C_6D_6), δ: 143.7. ^1H NMR (C_6D_6), δ: 1.21 (s, 9H, CH_3,S^{t}Bu), 1.30 (b, 2H, CH_2), 1.60 (s, 9H, CH_3, ^{t}Bu), 1.62 (b, 3H, CH_2), 1.66 (s, 9H, CH_3, ^{t}Bu), 1.70 (s, 3H, CH_3), 1.72 (s, 3H, CH_3), 1.93 (b, 2H, CH_2[1]), 2.04 (s, 3H, CH_3), 2.07 (s, 3H, CH_3), 2.32 (m, 1H, CH_2), 3.05 (b, CH-S), 4.76 (m, 1H, CH-O), 7.24 (s, 1H, CH=), 7.25 (s, 1H, CH=).^{13}C NMR (C_6D_6), δ: 16.2 (CH_3), 16.4 (CH_3), 19.5 (CH_2), 19.9 (CH_3), 20.0 (CH_3), 21.2 (CH_2), 27.8 (b, CH_2), 28.2 (b, CH_2), 30.8 (CH_3, S^{t}Bu), 31.2 (d, CH_3, ^{t}Bu, $J_{C\text{-}P}$= 5.5Hz), 31.6 (CH_3, ^{t}Bu), 34.5 (C, ^{t}Bu), 34.7 (C, ^{t}Bu), 43.0 (CH-S), 43.9 (C,S^{t}Bu), 76.1 (d, CH-O, $^2J_{C\text{-}P}$=14.7 Hz), 125.2-145.8 (aromatic carbons). Anal. calcd. (%) for $C_{34}H_{51}O_3PS$: C 71.54, H 9.01, S 5.62; found: C 71.52, H 8.99, S 5.58. MS HR-ESI [found 593.3187, $C_{34}H_{51}O_3PS$ $(M\text{-}Na)^+$ requires 593.3189].

L1e: Yield: 404 mg (70%). ^{31}P NMR (C_6D_6), δ: 133.6. ^1H NMR (C_6D_6), δ: 1.19 (s, 9H, CH_3, S^{t}Bu), 1.26 (b, 1H, CH_2), 1.56 (b, 1H, CH_2) 1.60 (s, 9H, CH_3, ^{t}Bu), 1.61 (s, 9H, CH_3, ^{t}Bu), 1.60-1.75 (b, 5H, CH_2), 1.69 (s, 3H, CH_3), 1.77 (s, 3H, CH_3), 2.05 (s, 3H, CH_3), 2.09 (s, 3H, CH_3), 2.27 (m, 1H, CH_2), 3.19 (m, 1H, CH-S), 4.48 (m, 1H, CH-O), 7.22 (s, 1H, CH=), 7.24 (s, 1H, CH=). ^{13}C NMR (C_6D_6), δ: 16.8 (CH_3), 17.2 (CH_3), 20.6 (CH_3), 20.7 (CH_3), 20.8 (CH_2), 22.6 (CH_2), 29.8 (CH_2), 30.3 (CH_2), 31.6 (CH_3, S^{t}Bu), 31.9 (d, CH_3, ^{t}Bu, $J_{C\text{-}P}$=5.6Hz), 32.1 (CH_3, ^{t}Bu), 35.2 (C, ^{t}Bu), 35.4 (C, ^{t}Bu), 43.6 (CH-S), 44.5 (C, S^{t}Bu), 77.6 (d, CH-O, $^2J_{C\text{-}P}$=2.1Hz), 128-146.7 (aromatic carbons). Anal. calcd. (%) for $C_{34}H_{51}O_3PS$: C 71.54, H 9.01, S 5.62; found: C 71.50, H 9.02, S 5.59. MS HR-ESI [found 593.3183, $C_{34}H_{51}O_3PS$ $(M\text{-}Na)^+$ requires 593.3189].

L2d: Yield: 392 mg (63%). ^{31}P NMR (C_6D_6), δ: 141.7. ^1H NMR (C_6D_6), δ: 1.19 (m, 1H, CH_2), 1.26 (m, 1H, CH_2), 1.49 (s, 9H, CH_3, ^{t}Bu), 1.56 (s, 9H, CH_3, ^{t}Bu), 1.57 (b, 3H, CH_2), 1.68 (s, 6H, CH_3), 1.89 (m, 1H, CH_2), 2.01 (b, 1H, CH_2), 2.03 (s, 3H, CH_3-Ph), 2.05 (s, 3H, CH_3-Ph), 2.19 (m, 1H, CH_2), 2.45 (s, 6H, CH_3), 3.20 (m, 1H, CH-S), 4.60 (m, 1H, CH-O), 6.93-7.20 (m, 5H, CH=).^{13}C NMR (C_6D_6), δ: 16.9 (CH_3), 17.1 (CH_3), 20.7 (CH_3), 21.2 (CH_2), 22.2 (CH_2), 22.9 (CH_3-Ph), 27.7 (b, CH_2), 29.3 (b, CH_2), 31.7 (d, CH_3, ^{t}Bu, $J_{C\text{-}P}$=5.3Hz), 32.6 (CH_3, ^{t}Bu), 35.0 (C, ^{t}Bu), 35.3 (C, ^{t}Bu), 52.2 (CH-S), 76.2 (d, CH-O, $^2J_{C\text{-}P}$= 15.3 Hz), 126.0-146.4 (aromatic carbons). Anal. calcd. (%) for $C_{38}H_{51}O_3PS$: C 73.75, H 8.32, S 5.18; found: C 73.72, H 8.31, S 5.16. MS HR-ESI [found 641.3186, $C_{38}H_{51}O_3PS$ $(M\text{-}Na)^+$ requires 641.3189].

L2e: Yield: 344 mg (56%). ^{31}P NMR (C_6D_6), δ: 137.0. ^1H NMR (C_6D_6), δ: 1.31 (m, 1H, CH_2), 1.42 (m, 1H, CH_2), 1.75 (m, 1H, CH_2), 1.81 (s, 9H, CH_3, ^{t}Bu),1.83 (s, 9H, CH_3, ^{t}Bu), 1.84 (b, 3H, CH_2), 1.94 (s, 3H, CH_3), 2.01 (s, 3H, CH_3), 2.18 (m, 2H, CH_2), 2.29 (s, 3H, CH_3), 2.33 (s, 3H, CH_3), 2.75 (s, 6H, CH_3-Ph), 3.51 (m, 1H, CH-S), 4.79 (m, 1H, CH-O), 7.17-7.50 (m, 5H, CH=). ^{13}C NMR (C_6D_6), δ: 16.2 (CH_3), 16.5 (CH_3), 20.0 (CH_3), 21.0 (CH_2), 21.2 (CH_2), 22.3 (CH_3-Ph), 28.3 (b, CH_2), 30.2 (b, CH_2), 31.2 (d, CH_3, ^{t}Bu, $J_{C\text{-}P}$=5.4Hz), 31.5 (CH_3, ^{t}Bu), 34.5 (C, ^{t}Bu), 34.7 (C, ^{t}Bu), 51.4 (CH-S), 75.2 (d, CH-O, $^2J_{C\text{-}P}$=1.8 Hz), 125.3-143.2 (aromatic carbons). Anal. calcd. (%) for $C_{38}H_{51}O_3PS$: C 73.75, H 8.32, S 5.18; found: C 73.72, H 8.30, S 5.15. MS HR-ESI [found 641.3184, $C_{38}H_{51}O_3PS$ $(M\text{-}Na)^+$ requires 641.3189].

General procedure for the preparation of the thioether-phosphinite ligands L2f-g. The corresponding thioether-hydroxyl compound (0.5 mmol) and DMAP (6.7 mg, 0.055 mmol) were dissolved in toluene (1 ml), and triethylamine was added (0.09 ml, 0.65 mmol) at r.t., followed by the addition of the corresponding chlorophosphine (0.55 mmol) via syringe. The reaction was stirred for 20 min at r.t. The solvent was removed *in vacuo*, and the product was purified by flash chromatography on alumina (toluene/NEt_3 = 100/1) to produce the corresponding ligand as a colorless oil.

L2f: Yield: 307 mg (73%). ^{31}P NMR (C_6D_6), δ: 108.8. ^1H NMR (C_6D_6), δ: 0.85 (m, 1H, CH_2), 1.01 (m, 1H, CH_2), 1.32 (m, 2H, CH_2), 1.44 (m, 2H, CH_2), 1.71 (m, 1H, CH_2), 2.02 (m, 1H, CH_2), 2.46 (s, 6H, CH_3-Ph), 3.17 (m, 1H, CH-S), 4.03 (m, 1H, CH-O), 6.9-7.7 (m, 13H, CH=). ^{13}C NMR (C_6D_6), δ: 22.2 (CH_3-Ph), 22.8 (b, CH_2), 23.7 (b, CH_2), 30.2 (b, CH_2), 32.5 (b, CH_2), 52.0 (CH-S), 81.1 (d, CH-O, $^2J_{C\text{-}P}$=21.4 Hz), 127.3-143.8 (aromatic carbons). Anal. calcd. (%) for $C_{26}H_{29}OPS$: C 74.26, H 6.95, S 7.62; found: C 74.33, H 6.96, S 7.59. MS HR-ESI [found 443.1563, $C_{26}H_{29}OPS$ $(M\text{-}Na)^+$ requires 443.1569].

L2g: Yield: 363 mg (81%). ^{31}P NMR (C_6D_6), δ: 95.2. ^1H NMR (C_6D_6), δ: 0.95 (m, 1H, CH_2), 1.09 (m, 1H, CH_2), 1.37 (m, 2H, CH_2), 1.49 (m, 2H, CH_2), 1.76 (m, 1H, CH_2), 2.05 (m, 1H, CH_2), 2.28 (s, 3H, CH_3-Ph), 2.38 (s, 3H, CH_3-Ph), 2.42 (s, 6H, CH_3-Ph), 3.09 (m, 1H, CH-S), 4.00 (m, 1H, CH-O), 6.8-7.8 (m, 11H, CH=). ^{13}C NMR (C_6D_6), δ: 20.2 (CH_3-Ph), 20.5 (CH_3-Ph), 22.1 (CH_3-Ph), 22.5 (b, CH_2), 23.3 (b, CH_2), 29.7 (b, CH_2), 31.6 (b, CH_2), 52.0 (CH-S), 80.1 (d, CH-O, $^2J_{C\text{-}P}$=16.2 Hz), 125.7-143.3 (aromatic carbons). Anal. calcd. (%) for $C_{28}H_{33}OPS$: C 74.97, H 7.41, S 7.15; found: C 75.08, H 7.42, S 7.10. MS HR-ESI [found 471.1878, $C_{28}H_{33}OPS$ $(M\text{-}Na)^+$ requires 471.1882].

General procedure for the preparation of [Ir(cod)(P-S)]BAr_F (P-S=L1-L2a-g). The corresponding ligand (0.074 mmol) was dissolved in CH_2Cl_2 (5 mL) and $[Ir(\mu\text{-}Cl)(cod)]_2$ (25.0 mg, 0.037 mmol) was added. The reaction mixture was refluxed at 50 °C for 1 hour. After 5 min at room temperature, $NaBAr_F$ (77.2 mg, 0.080 mmol) and water (5 mL) were added and the reaction mixture was stirred vigorously for 30 min at room temperature. The phases were separated and the aqueous phase was extracted twice with CH_2Cl_2. The combined organic phases were dried with $MgSO_4$, filtered through a plug of silica and the solvent was evaporated, resulting in the product as a red-orange solid.

[Ir(cod)(L1a)]BAr_F (3): Yield: 123 mg (93). ^{31}P NMR (C_6D_6), δ: 99.9. ^1H NMR (C_6D_6), δ: 1.33 (s, 9H, CH_3, ^{t}Bu), 1.36 (s, 9H, CH_3, ^{t}Bu), 1.49 (s, 9H, CH_3, ^{t}Bu), 1.52 (s, 9H, CH_3, ^{t}Bu), 1.61 (s, 9H, CH_3, S^{t}Bu), 1.76 (b, 2H, CH_2), 1.82 (b, 2H, CH_2), 1.95 (m, 2H, CH_2), 2.01 (m, 2H, CH_2, COD), 2.14 (m, 2H, CH_2), 2.21 (m, 2H, CH_2, COD), 2.30 (m, 2H, CH_2, COD), 2.38 (m, 2H, CH_2, COD), 2.72 (m, 1H, CH-S), 4.21 (m, 1H, CH-O), 4.61 (b, 1H, CH=, COD), 4.88 (m, 2H, CH=, COD), 5.76 (b, 1H, CH=, COD), 6.97-7.76 (m, 16H, CH=, Ar). ^{13}C NMR (C_6D_6), δ: 23.9 (CH_2), 25.8 (CH_2), 26.8 (b, CH_2, COD), 29.9 (b, CH_2, COD), 30.3 (b, CH_2, COD), 31.2 (CH_2), 31.3 (CH_3, ^{t}Bu), 31.4 (CH_3, ^{t}Bu), 31.5 (CH_3, ^{t}Bu), 31.5 (CH_3, ^{t}Bu), 32.0 (CH_3, S^{t}Bu), 33.6 (b, CH_2, COD), 34.9 (b, CH_2, COD), 35.7 (C, ^{t}Bu), 36.0 (C, ^{t}Bu), 47.6 (CH-S), 58.8 (C, S^{t}Bu), 77.4 (CH=, COD), 78.0 (CH-O), 78.0 (b, CH=, COD), 99.4 (d, $J_{C\text{-}P}$= 20.36 Hz, CH=, COD), 110.7 (d, $J_{C\text{-}P}$= 14.01 Hz, CH=, COD), 117.7 (b, CH=, BAr_F), 120.6-131.2 (aromatic carbons), 134.9 (b, CH=, BAr_F), 138.1-149.3 (aromatic carbons), 161.8 (q, $^1J_{C\text{-}B}$ = 49.4 Hz, C-B, BAr_F). Anal. calcd. (%) for $C_{78}H_{83}BF_{24}IrO_3PS$: C 52.32, H 4.67, S 1.79; found: C 52.29, H 4.66, S 1.75. MS HR-ESI [found 927.4487, $C_{46}H_{71}IrO_3PS$ $(M\text{-}BAr_F)^+$ requires 927.4491].

[Ir(cod)(L1b)]BAr_F (4): Yield: 116 mg (90%). ^{31}P NMR (C_6D_6), δ: 102.9. ^1H NMR (C_6D_6), δ: 1.44 (s, 9H, CH_3, ^{t}Bu), 1.51 (s, 9H, CH_3, ^{t}Bu), 1.59 (s, 9H, CH_3, ^{t}Bu), 1.79 (m, 4H, CH_2), 2.00 (m, 2H, CH_2, COD), 2.11

(m, 2H, CH_2, COD), 2.20 (m, 2H, CH_2), 2.12 (m, 2H, CH_2, COD), 2.29 (m, 2H, CH_2, COD), 2.32 (m, 2H, CH_2), 2.75 (m, 1H, CH-S), 3.80 (s, 3H, CH_3-O), 3.84 (s, 3H, CH_3-O), 4.24 (m, 1H, CH-O), 4.77 (b, 2H, CH=, COD), 4.91 (m, 1H, CH=, COD), 5.73 (b, 1H, CH=, COD), 6.52-7.70 (m, 16H, CH=, Ar). ^{13}C NMR (C_6D_6), δ: 23.8 (CH_2), 25.8 (CH_2) 27.2 (CH_2, COD), 29.9 (CH_2, COD), 30.7 (CH_2), 31.2 (CH_3, ^{t}Bu), 31.8 (CH_3, ^{t}Bu), 31.9 (CH_3, ^{t}Bu), 33.9 (b, CH_2, COD), 34.1 (b, CH_2, COD), 35.2 (CH_2), 35.9 (C, ^{t}Bu), 36.1 (C, ^{t}Bu), 47.7 (CH-S), 55.8 (CH_3-O), 55.9 (CH_3-O), 58.5 (C, S^{t}Bu), 75.8 (CH=, COD), 77.4 (CH-O), 79.5 (CH=, COD), 99.7 (d, $J_{C\text{-}P}$= 19.56 Hz, CH=, COD), 111.0 (d, $J_{C\text{-}P}$=13.30 Hz, CH=, COD), 112.9-115.6 (aromatic carbons), 117.6 (b, CH=, BAr_F), 120.6-131.9 (aromatic carbons), 135.0 (b, CH=, BAr_F), 140.4-157.3 (aromatic carbons), 161.9 (q, $^1J_{C\text{-}B}$ = 49.4 Hz, C-B, BAr_F). Anal. calcd. (%) for $C_{72}H_{71}BF_{24}IrO_5PS$: C 49.75, H 4.12, S 1.84; found: C 49.61, H 4.10, S 1.79. MS HR-ESI [found 875.3447, $C_{40}H_{59}IrO_5PS$ $(M\text{-}BAr_F)^+$ requires 875.3450].

[**Ir(cod)(L1c)**]**BAr$_F$ (5)**: Yield: 115 mg (91%). ^{31}P NMR (C_6D_6), δ: 99.0. ^{1}H NMR (C_6D_6), δ: 0.44 (s, 18H, CH_3, $SiMe_3$), 1.57 (s, 9H, CH_3, S^{t}Bu), 1.79 (b, 4H, CH_2, CH_3), 1.96 (m, 2H, CH_2, COD), 2.09 (m, 2H, CH_2, COD), 2.20 (m, 4H, CH_2 and CH_2, COD), 2.20 (m, 4H, CH_2 and CH_2, COD), 2.66 (m, 1H, CH-S), 4.14 (m, 1H, CH=, COD), 4.69 (b, 1H, CH=, COD), 4.92 (m, 2H, CH=, COD, CH-O), 5.90 (b, 1h, CH=, COD), 7.23-7.70 (m, 18H, CH=, Ar). ^{13}C NMR (C_6D_6), δ: 0.7 (CH_3, $SiMe_3$), 1.0 (CH_3, $SiMe_3$), 24.1 (CH_2), 25.9 (CH_2), 26.8 (CH_2, COD), 30.3 (CH_2, COD), 31.2 (CH_2), 31.7 (CH_3, S^{t}Bu), 33.4 (d, $J_{C\text{-}P}$= 6.25 Hz, CH_2, COD), 34.7 (d, $J_{C\text{-}P}$= 5.54 Hz, CH_2, COD), 34.9 (CH_2^1), 47.6 (CH-S), 58.8 (C, S^{t}Bu), 76.9 (CH=, COD), 77.4 (CH-O), 78.5 (CH=, COD), 99.9 (d, $J_{C\text{-}P}$= 20.36 Hz, CH=, COD), 111.6 (d, $J_{C\text{-}P}$= 14.11 Hz, CH=, COD), 117.6 (b, CH=, BAr_F), 120.7-133.1 (aromatic carbons), 134.9 (b, CH=, BAr_F), 135.8-154.1 (aromatic carbons), 161.9 (q, $^1J_{C\text{-}B}$ = 49.2 Hz, C-B, BAr_F). Anal. calcd. (%) for $C_{68}H_{67}BF_{24}IrO_3PSSi_2$: C 47.75, H 3.95, S 1.87; found: C 47.68, H 3.92, S 1.84. MS HR-ESI [found 847.2773, $C_{36}H_{55}IrO_3PSSi_2$ $(M\text{-}BAr_F)^+$ requires 847.2777].

[**Ir(cod)(L1d)**]**BAr$_F$ (6):** Yield: 119 mg (93%). ^{31}P NMR ($CDCl_3$), δ: 99.8. ^{1}H NMR ($CDCl_3$), δ: 1.38 (b, 2H, CH_2), 1.44 (s, 9H, CH_3, ^{t}Bu), 1.53 (s, 9H, CH_3, ^{t}Bu), 1.56 (m, 2H, CH_2), 1.57 (s, 9H, CH_3, ^{t}Bu), 1.64 (s, 3H, CH_3), 1.75 (b, 6H, CH_2), 1.84 (s, 3H, CH_3), 2.1-2.2 (b, 6H, CH_2), 2.23 (s, 3H, CH_3), 2.25 (s, 3H, CH_3), 2.69 (m, 1H, CH-S), 4.24 (m, 1H, CH=, COD), 4.36 (m, 1H, CH=, COD), 4.91 (m, 2H, CH=, COD and CH-O), 5.59 (m, 1H, CH=, COD), 7.17-7.70 (m, 14H, CH=, Ar). ^{13}C NMR ($CDCl_3$), δ: 16.4 (CH_3-Ph), 16.7 (CH_3-Ph), 20.3 (CH_3-Ph), 20.6 (CH_3-Ph), 23.7 (CH_2), 25.8 (CH_2), 27.8 (b, CH_2), 29.2 (CH_2), 31.2 (CH_3, ^{t}Bu), 31.2 (b, CH_2), 31.7 (CH_3, ^{t}Bu), 31.9 (CH_3, ^{t}Bu), 33.2 (b, CH_2), 34.7 (b, CH_2), 35.2 (C, ^{t}Bu), 35.3 (C, ^{t}Bu), 35.5 (C, ^{t}Bu), 47.7 (CH-S), 57.6 (C, S^{t}Bu), 74.1 (b, CH=, COD), 77.7 (b, CH=, COD), 81.6 (CH-O), 99.2 (d, $J_{C\text{-}P}$= 19.7 Hz, CH=, COD), 110.4 (d, $J_{C\text{-}P}$= 14.0 Hz, CH=, COD), 117.6 (b, CH=, BAr_F), 123.3-134.4 (aromatic carbons), 134.9 (b, CH=, BAr_F), 135.9-143.9 (aromatic carbons), 161.9 (q, $^1J_{C\text{-}B}$ = 49.4 Hz, C-B, BAr_F). Anal. calcd. (%) for $C_{74}H_{75}BF_{24}IrO_3PS$: C 51.25, H 4.36, S 1.85; found: C 51.05, H 4.34, S 1.82. MS HR-ESI [found 871.3861, $C_{42}H_{63}IrO_3PS$ $(M\text{-}BAr_F)^+$ requires 871.3865].

[**Ir(cod)(L1e)**]**BAr$_F$ (7):** Yield: 118 mg (92%). ^{31}P NMR (C_6D_6), δ: 94.6. ^{1}H NMR ($CDCl_3$), δ: 1.4-1.6 (b, 4H, CH_2), 1.40 (s, 9H, CH_3, ^{t}Bu), 1.56 (s, 9H, CH_3, ^{t}Bu), 1.6-1.9 (m, 6H, CH_2), 1.62 (s, 3H, CH_3), 1.64 (s, 9H, CH_3, ^{t}Bu), 1.85 (s, 3H, CH_3), 2.1-2.4 (b, 6H, CH_2), 2.25 (s, 3H, CH_3), 2.29 (s, 3H, CH_3), 2.81 (m, 1H, CH-S), 4.12 (m, 1H, CH=, COD), 4.55 (m, 1H, CH=, COD), 4.92 (m, 2H, CH=, COD and CH-O), 5.98 (m, 1H, CH=, COD), 7.12-7.70 (m, 14H, CH=, Ar). ^{13}C NMR ($CDCl_3$), δ: 16.7 (CH_3-Ph), 20.2 (CH_3-Ph), 20.7 (CH_3-Ph), 24.4 (CH_2), 25.1 (CH_2), 25.8 (b, CH_2), 30.1 (CH_2), 30.8 (CH_3, ^{t}Bu), 31.6 (b, CH_2), 32.0 (CH_3, ^{t}Bu), 32.2 (CH_3, ^{t}Bu), 33.7 (b, CH_2), 34.2 (b, CH_2), 34.7 (b, CH_2), 35.2 (C, ^{t}Bu), 36.4 (C, ^{t}Bu), 46.8 (CH-S), 57.9 (C, S^{t}Bu), 61.9 (b, CH=, COD), 63.4 (b, CH=, COD), 79.6 (CH-O), 97.6 (d, $J_{C\text{-}P}$= 18.4 Hz, CH=, COD), 110.2 (d, $J_{C\text{-}P}$= 16.1 Hz, CH=, COD), 117.7 (b, CH=, BAr_F), 120.6-134.6 (aromatic carbons), 134.9 (b, CH=, BAr_F), 137.2-144.2 (aromatic carbons), 161.8 (q, $^1J_{C\text{-}B}$ = 49.4 Hz, C-B, BAr_F). Anal. calcd. (%) for $C_{74}H_{75}BF_{24}IrO_3PS$: C 51.25, H 4.36, S 1.85; found: C 51.11, H 4.35, S 1.82. MS HR-ESI [found 871.3863, $C_{42}H_{63}IrO_3PS$ $(M\text{-}BAr_F)^+$ requires 871.3865].

[**Ir(cod)(L1f)**]**BAr$_F$ (8)**: Yield: 103 mg (91%). ^{31}P NMR (C_6D_6), δ: 100.9. ^{1}H NMR (C_6D_6), δ: 1.24 (s, 9H, CH_3, S^{t}Bu), 1.37 (m, 2H, CH_2), 1.49 (m, 2H, CH_2), 1.79 (m, 2H, CH_2, COD), 1.86 (m, 2H, CH_2), 2.03 (m, 2H, CH_2, COD), 2.17 (m, 2H, CH_2, COD), 2.28 (m, 2H, CH_2, COD), 2.37 (m, 2H, CH_2), 2.76 (m, 1H, CH-S), 3.37 (b, 1H, CH-O), 4.20 (m, 2H, CH=. COD), 4.81 (m, 1H, CH=, COD), 5.48 (b, 1H, CH=, COD), 7.16-7.70 (m, 22H, CH=, Ar). ^{13}C NMR (C_6D_6), δ: 24.3 (CH_2), 25.9 (CH_2), 28.0 (CH_2, COD), 31.3 (CH_3, S^{t}Bu), 31.8 (CH_2), 34.0 (CH_2, COD), 35.0 (CH_2, COD), 35.4 (CH_2), 48.7 (CH-S), 59.4 (C, S^{t}Bu), 74.7 (CH=, COD), 77.4 (CH-O), 83.3 (CH=, COD), 96.1 (d, $J_{C\text{-}P}$= 13.31 Hz, CH=, COD), 104.8 (d, $J_{C\text{-}P}$= 11.79 Hz, CH=, COD), 117.6 (b, CH=, BAr_F), 120.7-134.7 (aromatic carbons), 134.9 (b, CH=, BAr_F), 135.3 (C), 161.9 (q, $^1J_{C\text{-}B}$ = 49.2 Hz, C-B, BAr_F). Anal. calcd. (%) for $C_{62}H_{53}BF_{24}IrOPS$: C 48.48, H 3.48, S 2.09; found: C 48.21, H 3.46, S 2.02. MS HR-ESI [found 673.2239, $C_{30}H_{41}IrOPS$ $(M\text{-}BAr_F)^+$ requires 673.2245].

[**Ir(cod)(L2d)**]**BAr$_F$ (9)**: Yield: 125 mg (95%). ^{31}P NMR (C_6D_6), δ: 88.7. ^{1}H NMR (C_6D_6), δ:1.15 (m, 1H, CH_2), 1.27 (b, 1H, CH_2), 1.47 (s, 9H, CH_3, ^{t}Bu), 1.62 (m, 1H, CH_2), 1.64 (s, 9H, CH_3, ^{t}Bu), 1.74 (m, 2H, CH_2), 1.76 (s, 6H, CH_3), 1.84 (m, 3H, CH_2), 1.97 (m, 4H, CH_2 and CH_2, COD), 2.01 (m, 4H, CH_2 and CH_2, COD), 2.26 (s, 3H, CH_3), 2.27 (s, 3H, CH_3), 2.70 (s, 3H, CH_3), 2.72 (s, 3H, CH_3), 3.26 (b, 1H, CH-S), 3.53 (m, 1H, CH=, COD), 4.40 (m, 1H, CH=, COD), 4.54 (m, 2H, CH=, COD), 4.74 (m, 1H, CH-O), 7.20-7.71 (m, 17H, CH=, Ar). ^{13}C NMR (C_6D_6), δ: 16.6 (CH_3), 16.6 (CH_3), 20.3 (CH_3-Ph), 20.3 (CH_3-Ph), 23.6 (CH_3), 23.8 (CH_3), 25.4 (CH_2), 27.6 (b, CH_2, COD), 29.3 (CH_2), 29.7 (CH_2), 31.6 (CH_3, ^{t}Bu), 31.8 (b, CH_2, COD), 32.3 (CH_3, ^{t}Bu), 33.7 (b, CH_2, COD), 34.8 (b, CH_2), 34.9 (C, ^{t}Bu), 35.0 (C, ^{t}Bu), 50.9 (d, $J_{C\text{-}P}$= 5.44 Hz, CH=, COD), 66.9 (CH-S), 76.9 (CH-O), 82.1 (b, CH=, COD), 102.4 (d, $J_{C\text{-}P}$= 15.6 Hz, CH=, COD), 104.0 (d, $J_{C\text{-}P}$= 14.82 Hz, CH=, COD), 117.4 (b, CH=, BAr_F), 120.4-134.1 (aromatic carbons), 134.8 (b, CH=, BAr_F), 135.7-144.9 (aromatic carbons), 161.7 (q, $^1J_{C\text{-}B}$ = 49.0 Hz, C-B, BAr_F). Anal. calcd. (%) for $C_{78}H_{75}BF_{24}IrO_3PS$: C 52.56, H 4.24, S 1.80; found: C 52.34, H 4.22, S 1.77. MS HR-ESI [found 919.3858, $C_{46}H_{63}IrO_3PS$ $(M\text{-}BAr_F)^+$ requires 919.3865].

[**Ir(cod)(L2e)**]**BAr$_F$ (10)**: Yield: 122 mg (93%). ^{31}P NMR (C_6D_6), δ: 88.8. ^{1}H NMR (C_6D_6), δ: 1.38 (s, 9H, CH_3, ^{t}Bu), 1.55 (m, 2H, CH_2, COD), 1.57 (s, 9H, CH_3, ^{t}Bu), 1.66 (s, 3H, CH_3), 1.72 (b, 2H, CH_2), 1.75 (s, 3H, CH_3), 1.81 (m, 2H, CH_2, COD), 1.90-2.03 (m, 6H, CH_2), 2.10 (m, 2H, CH_2, COD), 2.17 (s, 3H, CH_3-Ph), 2.20 (s, 3H, CH_3-Ph), 2.25 (m, 2H, CH_2, COD), 2.42 (s, 3H, CH_3), 2.68 (m, 1H, CH-S), 2.88 (s, 3H, CH_3), 3.25 (m, 1H, CH=, COD), 3.81 (m, 1H, CH=, COD), 4.32 (m, 1H, CH=, COD), 4.46 (m, 1H, CH-O), 4.86 (m, 1H, CH=, COD), 7.07-7.64 (m, 17H, CH=, Ar). ^{13}C NMR (C_6D_6), δ: 16.4 (CH_3), 16.6 (CH_3), 20.3 (CH_3-Ph), 20.4 (CH_3-Ph), 22.6 (CH_3), 22.8 (CH_3), 25.4 (CH_2), 26.5 (b, CH_2, COD), 29.7 (CH_2), 29.9 (CH_2), 30.3 (CH_2), 31.4 (b, CH_2, COD), 31.7 (CH_3, ^{t}Bu), 32.8 (CH_3, ^{t}Bu), 34.2 (b, CH_2, COD), 34.6 (b, CH_2, COD), 34.8 (C, ^{t}Bu), 35.3 (C, ^{t}Bu), 52.6 (CH=, COD), 66.2 (CH-S), 76.2 (CH-O), 78.3 (b, CH=, COD), 102.3 (d, $J_{C\text{-}P}$= 14.11 Hz, CH=, COD), 105.3 (d, $J_{C\text{-}P}$= 16.43 Hz, CH=, COD), 117.5 (b, CH=, BAr_F), 120.4-134.4 (aromatic carbons), 134.8 (b, CH=, BAr_F), 135.4-143.5 (aromatic carbons), 161.5 (q, $^1J_{C\text{-}B}$ = 49.2 Hz, C-B, BAr_F). Anal. calcd. (%) for $C_{78}H_{75}BF_{24}IrO_3PS$: C 52.56, H 4.24, S 1.80; found: C 52.38, H 4.23, S 1.79. MS HR-ESI [found 919.3861, $C_{46}H_{63}IrO_3PS$ $(M\text{-}BAr_F)^+$ requires 919.3865].

[**Ir(cod)(L2f)**]**BAr$_F$ (11)**: Yield: 107 mg (91%). ^{31}P NMR (C_6D_6), δ: 99.0. ^{1}H NMR (C_6D_6), δ: 1.27 (b, 2H, CH_2), 1.56 (m, 2H, CH_2, COD), 1.68 (b, 2H, CH_2), 1.83 (m, 2H, CH_2, COD), 1.91 (m, 2H, CH_2, COD), 2.08 (m, 2H, CH_2, COD), 2.36 (m, 4H, CH_2), 2.63 (s, 3H, CH_3-Ph), 3.05 (s, 3H, CH_3-Ph), 3.12 (b, 1H, CH=, COD), 3.43 (m, 2H, CH-S, CH=, COD), 3.70 (b, 2H, CH-O, CH=, COD) 5.01 (b, 1H, CH=, COD), 7.17-

8.03 (m, 25H, CH=, Ar). ^{13}C NMR (C_6D_6), δ: 22.8 (CH_3-Ph), 23.5 (CH_3-Ph), 25.4 (CH_2), 27.5 (b, CH_2, COD), 29.7 (b, CH_2), 30.2 (CH_2), 30.3 (CH_2), 31.2 (b, CH_2, COD), 33.0 (b, CH_2, COD), 35.0 (b, CH_2, COD), 51.3 (CH=, COD), 67.4 (CH-S), 75.9 (CH-O), 77.8 (CH=, COD), 94.1 (d, $J_{C\text{-}P}$= 9.37 Hz, CH=, COD), 98.5 (d, $J_{C\text{-}P}$= 13.20 Hz, CH=, COD), 117.5 (b, CH=, BAr_F), 120.4-133.9 (aromatic carbons), 134.8 (b, CH=, BAr_F), 134.9-143.2 (aromatic carbons), 161.5 (q, $^1J_{C\text{-}B}$ = 49.4 Hz, C-B, BAr_F). Anal. calcd. (%) for $C_{66}H_{53}BF_{24}IrOPS$: C 50.04, H 3.37, S 2.02 found: C 49.98, H 3.35, S 1.98. MS HR-ESI [found 721.2240, $C_{34}H_{41}IrOPS$ (M-BAr_F)$^+$ requires 721.2245].

[**Ir(cod)(L2g)]BAr$_F$ (12)**: Yield: 112 mg (94%). ^{31}P NMR (C_6D_6), δ: 101.6. ^{1}H NMR (C_6D_6), δ: 1.40 (m , 2H, CH_2), 1.50 (m, 2H, CH_2), 1.61 (m, 2H, CH_2), 1.79-2.01 (m, 6H, CH_2 and CH_2, COD), 2.08 (s, 3H, CH_3), 2.17 (m, 4H, CH_2, COD), 2.41 (s, 3H, CH_3), 2.56 (b, 1H, CH=, COD), 2.82 (s, 3H, CH_3-Ph), 2.90 (s, 3H, CH_3-Ph), 3.08 (b, 1H, CH-S), 3.47 (m, 1H, CH=, COD), 3.66 (m, 2H, CH-O, CH=, COD), 4.70 (b, 1H, CH=, COD), 6.62-8.95 (m, 23H, CH=, Ar). ^{13}C NMR (C_6D_6), δ: 21.7 (d, $J_{C\text{-}P}$= 3.0 Hz, CH_3), 22.5 (d, $J_{C\text{-}P}$= 7.0 Hz, CH_3-Ph), 22.7 (d, $J_{C\text{-}P}$= 3.0 Hz, CH_3-Ph), 23.4 (b, CH_3), 25.5 (CH_2), 27.8 (b, CH_2, COD), 29.6 (CH_2), 29.7 (CH_2), 30.3 (CH_2), 31.2 (CH_2, COD), 33.0 (, CH_2, COD), 35.7 (d, $J_{C\text{-}P}$= 7.0 Hz, CH_2, COD), 50.8 (CH=, COD), 68.0 (CH-S), 76.5 (CH-O), 78.8 (b, CH=, COD), 96.9 (d, $J_{C\text{-}P}$= 9.4 Hz, CH=, COD), 98.1 (d, $J_{C\text{-}P}$= 13.3 Hz, CH=, COD), 117.5 (b, CH=, BAr_F), 120.5-133.9 (aromatic carbons), 134.8 (b, CH=, BAr_F), 139.9-143.4 (aromatic carbons), 161.5 (q, $^1J_{C\text{-}B}$ = 49.2 Hz, C-B, BAr_F). Anal. calcd. (%) for $C_{68}H_{57}BF_{24}IrOPS$: C 50.66, H 3.56, S 1.99 found: C 50.34, H 3.53, S 1.93. MS HR-ESI [found 749.2553, $C_{36}H_{45}IrOPS$ (M-BAr_F)$^+$ requires 749.2558].

In situ preparation of [Ir(H)$_2$(cod)(L1-L2a-g)]BAr$_F$. In a typical experiment hydrogen was bubbled through a CD_2Cl_2 solution of the desired [Ir(cod)(P-S)]BAr_F catalyst precursor (6.2 mmol) to the desired temperature for 15-30 min. The reaction mixture was analyzed by NMR spectroscopy at the desired temperature.

In situ HP-NMR hydrogenation experiments using (E)-1-methyl-4-(1-phenylprop-1-en-2-yl)benzene-D5 19. The desired [Ir(cod)(P-S)]BAr_F catalyst precursor (6.2 μmol) and (*E*)-1-methyl-4-(1-phenylprop-1-en-2-yl)benzene-D5 (5.9 mg, 27.7 μmol, 4.5 equiv.) were added to an oven-dried Schlenk tube and dissolved in CD_2Cl_2 (0.6 ml). The solution was transferred to a HPNMR sapphire tube (ϕ = 5 mm) and cooled to 195 K. The HPNMR was pressurized to the desired pressure of hydrogen gas. The reaction mixture was analyzed by NMR spectroscopy at the desired temperature.

Typical procedure for the hydrogenation of olefins. The alkene (0.5 mmol) and Ir complex (2 mol%) were dissolved in CH_2Cl_2 (2 mL) in a high-pressure autoclave, which was purged four times with hydrogen. It was then pressurized at the desired pressure. After the desired reaction time, the autoclave was depressurized and the solvent evaporated off. The residue was dissolved in Et_2O (1.5 ml) and filtered through a short celite plug. The enantiomeric excess was determined by chiral GC or chiral HPLC and conversions were determined by ^{1}H NMR. The enantiomeric excesses of hydrogenated products from **S1**,[11] **S2**,[37] **S3-S4**,[11] **S5**,[38] **S6**,[11] **S7-S9**,[6l] **S10**,[39] **S11**,[40] **S12**,[38] **S13**,[39] **S14-S17**,[6i] **S18**,[20a] **S19**,[21d] **S20**,[21a] **S21**,[11] **S22**,[7c] **S23**,[36] **S24**,[11] **S25-S31**,[41] **S32**,[11] **S33-S37**,[21a] **S38**,[42] **S39**[43] and **S40**[44] were determined using the conditions previously described.

ASSOCIATED CONTENT

Supporting Information

Copies of ^{31}P{^{1}H}, ^{1}H and ^{13}C{^{1}H} NMR spectra, full set of catalytic results, enantiomeric excess determination and characterization details of hydrogenated products and ^{1}H NMR and mass spectra of the deuterium experiments (PDF).

CIF file of [Ir(**L1a**)(cod)]BAr_F complex **3** (CIF).

Calculated energies and coordinates for all computational structures (PDF).

The supplemental file CartCoord contains the computed Cartesian coordinates of all of the molecules reported in this study (xyz).

This material is available free of charge via Internet at http://pubs.acs.org.

AUTHOR INFORMATION

Corresponding Author

* Email: oscar.pamies@urv.cat.

* Email: montserrat.dieguez@urv.cat

Notes

The authors declare no competing financial interest

ACKNOWLEDGMENT

Financial support from the Spanish Government (CTQ2013-40568P), the Catalan Government (2014SGR670), the ICREA Foundation (ICREA Academia awards to M. Diéguez and O. Pàmies) is gratefully acknowledged.

REFERENCES

(1) (a) Balser, H.-U., Federsel, H.-J., Eds; *Asymmetric Catalysis in Industrial Scale: Challenges, Approaches and Solutions*, 2nd Ed; Wiley: Weinheim, **2010**. (b) Ojima, I., Ed; *Catalytic Asymmetric Synthesis*, 3rd Ed; John Wiley & Sons, Inc.: Hoboken, **2010**. (c) Jacobsen, E. N., Pfaltz, A., Yamamoto, H., Eds; *Comprehensive Asymmetric Catalysis*; Springer-Verlag: Berlin, **1999**.

(2) (a) Brown, J. M. In *Comprehensive Asymmetric Catalysis*; Jacobsen, E. N., Pfaltz, A., Yamamoto, H., Eds; Springer-Verlag: Berlin, **1999**; Vol. I, pp 121-182. (b) Noyori, R. *Asymmetric Catalysis in Organic Synthesis*; Wiley: New York, **1994**. (c) Wang, D.-S.; Chen, Q.-A.; Lu, S.-M.; Zhou, Y.-G. *Chem. Rev.* **2012**, *112*, 2557-2590. (d) Knowles, W. S.; Noyori, R. *Acc. Chem. Res.* **2007**, *40*, 1238-1239.

(3) (a) Genêt, J. P. In *Modern Reduction Methods*; Andersson, P. G., Munslow, I. J., Eds.; Wiley-VCH: Weinheim, **2008**. (b) Chi, Y., Tang, W., Zhang, X. In *Modern Rhodium-Catalyzed Organic Reactions*; Evans, P. A. Eds.; Wiley-VCH: Weinheim, **2005**. (c) Kitamura, M., Noyori, R. in *Ruthenium in Organic Synthesis*; Murahashi, S.-I., Ed.; Wiley-VCH: Weinheim, **2004**. (d) Tang, W.; Zhang, X. *Chem. Rev.* **2003**, *103*, 3029-3069. (e) Johnson, N. B.; Lennon, I. C.; Moran, P. H.; Ramsden, J. A. *Acc. Chem. Res.* **2007**, *40*, 1291-1299. (f) Weiner, B.; Szymanski, W.; Janssen, D. B.; Minnaard, A. J.; Feringa, B. L. *Chem. Soc. Rev.* **2010**, *39*, 1656-1691.

(4) For reviews, see: a) Cui, X.; Burgess, K. *Chem. Rev.* **2005**, *105*, 3272-3296. (b) Källström, K.; Munslow, I.; Andersson, P. G. *Chem. Eur. J.* **2006**, *12*, 3194-3200. (c) Roseblade, S. J.; Pfaltz, A. *Acc. Chem. Res.* **2007**, *40*, 1402-1411. (d) Church, T. L.; Andersson, P. G. *Coord. Chem. Rev.* **2008**, *252*, 513-531. (e) Pàmies, O.; Andersson, P. G.; Diéguez, M. *Chem. Eur. J.* **2010**, *16*, 14232-14240. (f) Woodmansee, D. H.; Pfaltz, A. *Chem. Commun.* **2011**, *47*, 7912-7916. g) Zhu, Y.; Burgess, K. *Acc. Chem. Res.* **2012**, *45*, 1623-1636. (h) Verendel, J. J.; Pàmies, O.; Diéguez, M.; Andersson, P. G. *Chem. Rev.* **2014**, *114*, 2130-2169.

(5) Lightfoot, A.; Schnider, P.; Pfaltz, A. *Angew. Chem. Int. Ed.* **1998**, *37*, 2897-2899.

(6) See, for instance: a) Blankenstein, J.; Pfaltz, A. *Angew. Chem. Int. Ed.* **2001**, *40*, 4445-4477. (b) Hou, D.-R.; Reibenspies, J. H.; Colacot, T. J.; Burgess, K. *Chem. Eur. J.* **2001**, *7*, 5391-5400. (c) Menges, F.; Pfaltz, A. *Adv. Synth. Catal.* **2002**, *344*, 40-44. (d) Perry, M. C.; Cui, X.; Powell, M. T.; Hou, D.-R.; Reibenspies, J. H.; Burgess, K. *J. Am. Chem. Soc.* **2003**, *125*, 113-123. (e) Tang, W.; Wang, W.; Zhang, X. *Angew. Chem. Int. Ed.* **2003**, *42*, 943-946. (f) Liu, D.; Tang, W.; Zhang, X. *Org. Lett.* **2004**, *6*, 513-516. (g) McIntyre, S.; Hörmann, E.; Menges, F.; Smidt, S. P.; Pfaltz, A. *Adv. Synth. Catal.* **2005**, *347*, 282-288. (h) Trifonova, A.; Diesen, J. S.; Anders-

son, P. G. *Chem. Eur. J.* **2006**, *12*, 2318-2328. (i) Lu, S.-M.; Bolm, C. *Angew. Chem. Int. Ed.* **2008**, *47*, 8920-8923. (j) Engman, M.; Cheruku, P.; Tolstoy, P.; Bergquist, J.; Völker, S. F.; Andersson, P. G. *Adv. Synth. Catal.* **2009**, *351*, 375-378. (k) Zhao, J.; Burgess, K. *J. Am. Chem. Soc.* **2009**, *131*, 13236-13237. (l) Lu, W.-J.; Chen, Y.-W.; Hou, X.-L. *Adv. Synth. Catal.* **2010**, *352*, 103-107. (m) Zhang, Y.; Han, Z.; Li, F.; Ding, K.; Zhang, A. *Chem. Commun.* **2010**, *46*, 156-158. (n) Verendel, J. J.; Zhou, T.; Li, J.-Q.; Paptchikhine, A.; Lebedev, O.; Andersson, P. G. *J. Am. Chem. Soc.* **2010**, *132*, 8880-8881. (o) Franzke, A.; Pfaltz, A. *Chem. Eur. J.* **2011**, *17*, 4131-4144. (p) Shang, J.; Han, Z.; Li, Y.; Wang, X.; Ding, K. *Chem. Commun.* **2012**, *48*, 5172-5174. (q) Wang, X.; Han, Z.; Wang, Z.; Ding, K. *Angew. Chem. Int. Ed.* **2012**, *51*, 936-940. (r) Verendel, J. J.; Li, J.-Q.; Quan, X.; Peters, B.; Zhou, T.; Gautun, O. R.; Govender, T.; Andersson, P. G. *Chem. Eur. J.* **2012**, *18*, 6507-6513. (s) Mazuela, J.; Pàmies, O.; Diéguez, M. *Eur. J. Inorg. Chem.* **2013**, 2139-2145. (t) Khumsubdee, S.; Fan, Y.; Burgess, K. *J. Org. Chem.* **2013**, *78*, 9969-9974. (u) Zhu, Y.; Burgess, K. *RSC Advances* **2012**, *2*, 4728-4735. (v) Müller, M.-A.; Pfaltz, A. *Angew. Chem Int. Ed.* **2014**, *53*, 8668-8671.

(7) (a) Diéguez, M.; Mazuela, J., Pàmies, O., Verendel, J. J., Andersson, P. G. *J. Am. Chem. Soc.* **2008**, *130*, 7208-7209. (b) Diéguez, M.; Pàmies, O.; Verendel, J. J.; Andersson, P. G. *Chem. Commun.* **2008**, 3888-3890. (c) Mazuela, J.; Verendel, J. J.; Coll, M.; Schäffner, B.; Börner, A.; Andersson, P. G.; Pàmies, O.; Diéguez, M. *J. Am. Chem. Soc.* **2009**, *131*, 12344-12353. (d) Mazuela, J.; Paptchikhine, A.; Pàmies, O.; Andersson, P. G.; Diéguez, M. *Chem. Eur. J.* **2010**, 16, 4567-4576. (e) Mazuela, J.; Norrby, P.-O.; Andersson, P. G.; Pàmies, O.; Diéguez, M. *J. Am. Chem. Soc.* **2011**, *133*, 13634-13645. (f) Mazuela, J.; Pàmies, O.; Diéguez, M. *Adv. Synth. Catal.* **2013**, *355*, 2569-2583. (g) Mazuela, J.; Pàmies, O.; Diéguez, M. *ChemCatChem* **2013**, *5*, 2410-2417. (h) van Leeuwen, P. W. N. M.: Kamer, P. C. J.: Claver, C.: Pàmies, O.; Diéguez, M. *Chem. Rev.* **2011**, *111*, 2077-2118.

(8) See, for example: (a) Bunlaksananusorn, T.; Polborn, K.; Knochel, P. *Angew. Chem. Int. Ed.* **2003**, *42*, 3941-3943. (b) Drury III, W. J.; Zimmermann, N.; Keenan, M.; Hayashi, M.; Kaiser, S.; Goddard, R.; Pfaltz, A. *Angew. Chem. Int. Ed.* **2004**, *43*, 70-74. (c) Bell, S.; Wüstenberg, B.; Kaiser, S.; Menges, F.; Netscher, T.; Pfaltz, A. *Science* **2006**, *311*, 642-644. (d) Kaiser, S.; Smidt, S. P.; Pfaltz, A. *Angew. Chem. Int. Ed.* **2006**, *45*, 5194-5197. (e) Margalef, J.; Lega, M.; Ruffo, F.; Pàmies, O.; Diéguez, M. *Tetrahedron: Asymmetry* **2012**, *23*, 945-951. (f) Woodmansee, D. H.; Müller, M.-A.; Tröndlin, L.; Hörmann, E.; Pfaltz, A. *Chem. Eur. J.* **2012**, *18*, 13780-13786. (g) Schumacher, A.; Bernasconi, M.; Pfaltz, A. *Angew. Chem. Int. Ed.* **2013**, *52*, 7422-7425. (h) Bernasconi, M.; Müller, M.-A.; Pfaltz, A. *Angew. Chem. Int. Ed.* **2014**, *53*, 5385-5388.

(9) Rageot, D.; Woodmansee, D. H.; Pugin, B.; Pfaltz A. *Angew. Chem. Int. Ed.* **2011**, *50*, 9598-9601.

(10) (a) Hedberg, C.; Källström, K.; Brandt, P.; Hansen, L. K.; Andersson, P. G. *J. Am. Chem. Soc.* **2006**, *128*, 2995-3001. (b) Källström, K.; Andersson, P. G. *Tetrahedron Lett. 2006*, 47, 7471-7480. (c) Engman, M.; Diesen, J. S.; Paptchikhine, A.; Andersson, P. G. *J. Am. Chem. Soc.* **2007**, *129*, 4536-4537. (d) Cheruku, P.; Paptchikhine, A.; Ali, M.; Neudoerfl, J.-M.; Andersson, P. G. *Org. Biomol. Chem.* **2008**, *6*, 366-373. (e) Cheruku, P.; Paptchikhine, A.; Church, T. L.; Andersson, P. G. *J. Am. Chem. Soc.* **2009**, *131*, 8285-8289. (f) Tolstoy, P.; Engman, M.; Paptchikhine, A.; Bergquist, J.; Church, T. L.; Leung, A. W.-M.; Andersson, P. G. *J. Am. Chem. Soc.* **2009**, *131*, 8855-8860. (g) Li, J.-Q.; Paptchikhine, A.; Govender, T.; Andersson, P. G. *Tetrahedron: Asymmetry* **2010**, *21*, 1328-1333. (h) Paptchikhine, A.; Itto, K.; Andersson, P. G. *Chem. Commun.* **2011**, *47*, 3989-3991. (i) Li, J.-Q.; Quan, X.; Andersson, P. G. *Chem. Eur. J.* **2012**, *18*, 10609-10616. (j) Zhou, T.; Peters, B.; Maldonado, M. F.; Govender, T.; Andersson, P. G. *J. Am. Chem. Soc.* **2012**, *134*, 13592-13595. (k) Yotapan, N.; Paptchikhine, A.; Bera, M.; Avula, S. K.; Vilaivan, T.; Andersson, P. G. *Asian J. Org. Chem.* **2013**, *2*, 674-680.

(11) Källström, K.; Hedberg, C.; Brandt, P.; Bayer, A.; Andersson, P. G. *J. Am. Chem. Soc.* **2004**, *126*, 14308-14309.

(12) (a) Coll, M.; Pàmies, O.; Diéguez, M. *Chem. Commun.* **2011**, *47*, 9215-9217. (b) Coll, M.; Pàmies, O.; Diéguez, M. *Adv. Synth. Catal.* **2013**, *355*, 143-160. (c) Margalef, J.; Caldentey, X.; Karlsson, E. A.; Coll, M.; Mazuela, J.; Pàmies, O.; Diéguez, M.; Pericàs, M. A. *Chem. Eur. J.* **2014**, *20*, 12201-12214. (d) Biosca, M.; Coll, M.; Lagarde, F.; Brémond, E.; Routaboul, L.; Manoury, E.; Pàmies, O.; Poli, R.; Diéguez, M. *Tetrahedron* **2015**, http://dx.doi.org/10.1016/j.tet.2015.01.047.

(13) The new phosphite-thioether ligands **L1**-**L2a-e** are similar to already known phosphinite-thioether ligands **L1f-g**, developed by Evans and coworkers, but with a π-acceptor biaryl phosphite group in lieu of the phosphinite moiety. Ligands **L1f-g** proved to be highly efficient in the enantioselective Rh-catalyzed hydrogenation of model functionalized substrates (dehydroamino acids), Rh-catalyzed hydrosilylation and Pd-catalyzed allylic substitution reactions. See: (a) Evans, D. A.; Campos, K. R.; Tedrow, J. S.; Michael, F. E.; Gagne, M. R. *J. Org. Chem.* **1999**, *64*, 2994-2995. (b) Evans, D. A.; Campos, K. R.; Tedrow, J. S.; Michael, F. E.; Gagne, M. R. *J. Am. Chem. Soc.* **2000**, *122*, 7905-7920. (c) Evans, D. A.; Michael, F. E.; Tedrow, J. S.; Campos, K. R. *J. Am. Chem. Soc.* **2003**, *125*, 3534-3543.

(14) Iida, T.; Yamamoto, N.; Sasai, H.; Shibasaki, M. *J. Am. Chem. Soc.* **1997**, *119*, 4783-4784.

(15) Pàmies, O.; Diéguez, M.; Net, G.; Ruiz, A.; Claver, C. *Organometallics* **2000**, *19*, 1488-1496.

(16) Evans and coworkers have already shown the important role of the spatial disposition of the thioether substituent (pseudoaxial) in analogous phosphinite-thioether ligands for the Rh-catalyzed hydrogenation of dehydro aminoacids, see ref. 13c.

(17) Schäffner, B.; Schäffner, F.; Verevkin, S. P.; Börner, A. *Chem. Rev.* **2010**, *110*, 4554-4581.

(18) For recent successful applications, see: (a) ref 10i. (b) ref 8f.

(19) Chiral carboxylic esters can also be obtained by asymmetric conjugated reduction of α,β-unsaturated esters with $NaBH_4$ using Co-catalysts and by the asymmetric 1,4-reduction with moisture-sensitive hydrosilane reagents using Rh- and Cu-catalysts. See for instance: (a) Leutenegger, U.; Madin, A.; Pfaltz, A. *Angew. Chem. Int. Ed. Engl.* **1989**, *28*, 60-61. (b) Yamada, T. M; Ohtsuka, Y.; Ikeno, T. *Chem. Lett.* **1998**, 1129-1130. (c) Appella, D. H.; Moritani, Y.; Shintani, R.; Ferreira, E. M.; Buchwald, S. L. *J. Am. Chem. Soc.* **1999**, *121*, 9473-9474. (d) Hughes, G.; Kimura, M.; Buchwald, S. L. *J. Am. Chem. Soc.* **2003**, *125*, 11253-11258. (e) Tsuchiya, Y.; Kanazwa, Y.; Shiomo, T.; Kobayashi, K.; Nishiyama, H. *Synlett* **2004**, 2493-2496.

(20) (a) Lu, W.-J.; Chen, Y.-W.; Hou, X.-L. *Angew. Chem., Int. Ed.* **2008**, *47*, 10133-10136. (b) Maurer, F.; Huch, V.; Ullrich, A.; Kazmaier, U. *J. Org. Chem.* **2012**, *77*, 5139-5143. (c) ref 6i. (d) ref 6q. (e) ref 6r.

(21) For successful application, see: (a) Lu, W.-J.; Hou, X.-L. *Adv. Synth. Catal.* **2009**, *351*, 1224-1228. (b) ref 6p.

(22) For successful applications, see: (a) Ganić, A.; Pfaltz, A. *Chem. Eur. J.* **2012**, *18*, 6724-6728. (b) ref 12c. (c) ref 7c. (d) Paptchikhine, A.; Cheruku, P.; Engman, M.; Andersson, P. G. *Chem. Commun.* **2009**, 5996-5998.

(23) It has been suggested that this isomerization process can proceed either via the formation of Ir-π-allyl intermediates or via protonation of the double bond at the terminal position, which gives a stabilized carbocation. (a) ref 6d; (b) Brown, J. M.; Derome, A. E.; Hughes, G. D.; Monaghan, P. K. *Aust. J. Chem.* **1992**, *45*, 143-153.

(24) (a) Brandt, P.; Hedberg, C.; Andersson, P. G. *Chem. Eur. J.* **2003**, *9*, 339-347. (b) Fan, Y.; Cui, X.; Burgess, K.; Hall, M. B. *J. Am. Chem. Soc.* **2004**, *126*, 16688-16689. (c) Cui, X.; Fan, Y.; Hall, M. B.; Burgess, K. *Chem. Eur. J.* **2005**, *11*, 6859-6868. (d) Church, T. L.; Rasmussen, T.; Andersson, P. G. *Organometallics* **2010**, *29*, 6769-6781. (e) Hopmann, K. H.; Bayer, A. *Organometallics* **2011**, *30*, 2483-2497. (f) ref 7e.

(25) Gruber, S.; Pfaltz, A. *Angew. Chem. Int. Ed.* **2014**, *53*, 1896-1900.

(26) Mazet, C.; Smidt, S. P.; Meuwly, M.; Pfaltz, A. *J. Am. Chem. Soc.* **2014**, *126*, 14176-14181.

(27) See for instance: a) Chodosh, D. F.; Crabtree, R. H.; Felkin, H.; Morris, G. E. *J. Organomet. Chem.* **1978**, *161*, C67-C70. b) Smidt, S. P.; Pfaltz, A.; Martínez-Viviente, E.; Pregosin, P. S.; Albinati, A. *Organometallics* **2003**, *22*, 1000-1009.

(28) Trinuclear iridium complexes **17** and **18** evolve with time to the formation of a new hydrido species, which have been attributed to the dinuclear iridium hydride $[IrH(CH_2Cl_2)(P\text{-}S)(\mu\text{-}H)](BAr_F)_2$ complexes (characteristic data for $[IrH(CH_2Cl_2)(\textit{ent}\text{-}\mathbf{L2d})(\mu\text{-}H)](BAr_F)_2$: $^{31}P_{Major}$ NMR (CD_2Cl_2), δ: 89.7. $^{1}H_{Major}$ NMR (CD_2Cl_2), δ: -14.58 (d, $^{2}J_{P\text{-}H}$= 6.4 Hz) and -27.56 (d, $^{2}J_{P\text{-}H}$= 32.4 Hz); $^{31}P_{Minor}$ NMR (CD_2Cl_2), δ: 87.6. $^{1}H_{Minor}$ NMR (CD_2Cl_2), δ: -14.58 (d, $^{2}J_{P\text{-}H}$= 6.4 Hz) and -27.72 (d, $^{2}J_{P\text{-}H}$= 30.6 Hz). Characteristic data for $[IrH(CH_2Cl_2)(\ \mathbf{L2e})(\mu\text{-}H)](BAr_F)_2$: ^{31}P NMR ($CD_2Cl_2$), δ: 87.5. ^{1}H NMR ($CD_2Cl_2$), δ: -15.61 (d, $^{2}J_{P\text{-}H}$= 6.8 Hz) and -27.41 (b); see Supporting Information). Gruber, S.; Neuburger, M.; Pfaltz, A. *Organometallics* **2013**, *32*, 4702-4711.

(29) Buisman, G. J. H.; Kamer, P. C. J.; van Leeuwen, P. W. N. M. *Tetrahedron: Asymmetry* **1993**, *4*, 1625-1634.

(30) Frisch, M. J.; Trucks, G. W.; Schlegel, H. B.; Scuseria, G. E.; Robb, M. A.; Cheeseman, J. R.; Scalmani, G.; Barone, V.; Mennucci, B.; Petersson, G. A.; Nakatsuji, H.; Caricato, M.; Li, X.; Hratchian, H. P.; Izmaylov, A. F.; Bloino, J.; Zheng, G.; Sonnenberg, J. L.; Hada, M.; Ehara, M.; Toyota, K.; Fukuda, R.; Hasegawa, J.; Ishida, M.; Nakajima, T.; Honda, Y.; Kitao, O.; Nakai, H.; Vreven, T.; Montgomery, J. A.; Peralta, J. E., Jr.; Ogliaro, F.; Bearpark, M.; Heyd, J. J.; Brothers, E.; Kudin, K. N.; Staroverov, V. N.; Kobayashi, R.; Normand, J.; Raghavachari, K.; Rendell, A.; Burant, J. C.; Iyengar, S. S.; Tomasi, J.; Cossi, M.; Rega, N.; Millam, J. M.; Klene, M.; Knox, J. E.; Cross, J. B.; Bakken, V.; Adamo, C.; Jaramillo, J.; Gomperts, R.; Stratmann, R. E.; Yazyev, O.; Austin, A. J.; Cammi, R.; Pomelli, C.; Ochterski, J. W.; Martin, R. L.; Morokuma, K.; Zakrzewski, V. G.; Voth, G. A.; Salvador, P.; Dannenberg, J. J.; Dapprich, S.; Daniels, A. D.; Farkas, O.; Foresman, J. B.; Ortiz, J. V.; Cioslowski, J.; Fox, D. J. Revision A.02 ed; Gaussian: Wallingford, CT, 2009.

(31) (a) Lee, C.; Yang,W.; Parr, R. G. *Phys. Rev*. B **1988**, *37*, 785-789. (b) Becke, A. D. *J. Chem. Phys*. **1993**, *98*, 5648-5652.

(32) Hay, P. J.; Wadt, W. R. *J. Chem. Phys.* **1985**, *82*, 299-310.

(33) (a) Hehre, W. J.; Ditchfield, R.; Pople, J. A. *J. Chem. Phys.* **1972**, *56*, 2257-2261. (b) Hariharan, P. C.; Pople, J. A. Theor. *Chim. Acta* **1973**, *28*, 213-222. (c) Francl, M. M.; Pietro,W. J.; Hehre,W. J.; Binkley, J. S.; Gordon, M. S.; Defrees, D. J.; Pople, J. A. *J. Chem. Phys*. **1982**, *77*, 3654-3665.

(34) (a) Miertus, S.; Tomasi, *J. Chem. Phys.* **1982**, *65*, 239-245. (b) Mennucci, B.; Tomasi, J. *J. Chem. Phys.* **1997**, *106*, 5151-5158. (c) Cossi, M.; Barone, V.; Menucci, B.; Tomasi, J. *Chem. Phys. Lett*. **1998**, *286*, 253-260.

(35) (a) Krishnan, R.; Binkley, J. S.; Seeger, R.; Pople, J. A. *J. Chem. Phys.* **1980**, *72*, 650-654. (b) McLean, A. D.; Chandler, G. S. *J. Chem. Phys.* **1980**, *72*, 5639-5648.

(36) (a) Grimme, S.; Antony, J.; Ehrlich, S.; Krieg, H. *J. Chem. Phys.* **2010**, *132*, 15410-15417. (b) Grimme, S.; Ehrlich, S.; Goerigk, L. *J. Comput. Chem.* **2011**, *32*, 1456-1465.

(37) Ohta, H. Ikegami, T. Miyake, H. Takaya, *J. Organomet. Chem.* **1995**, *502*, 169-176.

(38) Woodmansee, D. H.; Müller, M.-A.; Neuburger, M.; Pfaltz, A. *Chem. Sci.* **2010**, *1*, 72-78.

(39) Hou, C.-J.; Guo, W.-L.; Hu, X.-P.; Deng, J.; Zheng, Z. *Tetrahedron: Asymmetry* **2011**, *22*, 195-199.

(40) Giese, B.; Lachhein, S. *Chem. Ber*. **1985**, *118*, 1616-1620.

(41) Biosca, M.; Paptchikhine, A.; Pàmies, O.; Andersson, P. G.; Diéguez, M. *Chem. Eur. J*. **2015**, *21*, 3455-3464.

(42) Coll, M.; Pàmies, O.; Adolfsson, H.; Diéguez, M. *Chem. Commun.* **2011**, *47*, 12188-12190.

(43) Pastor, I. M.; Vastila, P.; Adolfsson, H. *Chem. Eur. J*. **2003**, *9*, 4031-4045.

(44) Sokeirik, Y. S.; Mori, H.; Omote, M.; Sato, K.; Tarui, A.; Kumadaki, I.; Ando, A. *Org. Lett.* **2007**, *9*, 1927-1929.

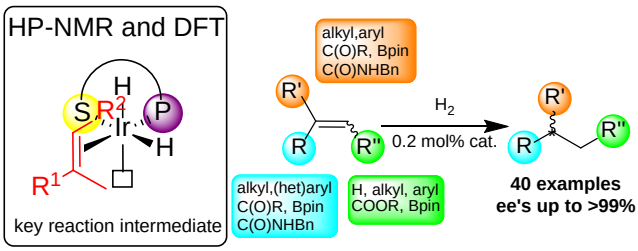
HP-NMR and DFT
H
S
R2
P
Ir
H
R1
key reaction intermediate
alkyl,aryl
C(O)R, Bpin
C(O)NHBn
R'
R
R''
H2
0.2 mol% cat.
alkyl,(het)aryl
C(O)R, Bpin
C(O)NHBn
H, alkyl, aryl
COOR, Bpin
40 examples
ee's up to >99%